Final Report

Dallas Field Study (DFS); Ozone Precursors, Local Sources and Remote Transport Including Biomass Burning

AQRP Project #: 22-010

QA Requirements: Audits of Data Quality: 10% Required

Project Participants: Aerodyne Research, Inc.

Prepared by: Edward Fortner

Aug 31, 2023

Executive Summary: Preliminary Findings

During the Dallas Field Study the Aerodyne Mobile Laboratory (AML) sampled over 50 point sources in the Dallas - Fort Worth (DFW) area and gained a wealth of information regarding the chemical speciation of the gas and particle phase emissions from those facilities. The AML also conducted upwind/downwind measurements of the DFW metro area on 4 days and gained a wealth of data characterizing an airmass prior to entering DFW and after exiting the metropolitan area. The third mission strategy which occurred on one measurement day was the measurement of a wildfire.

Sample of point source issues of concern:

Plumes of the Volatile Organic Compound (VOC) $C_{10}H_{17}$ found emitting from a home building company in Hillsboro. There are multiple compounds with this chemical structure which is why it is unnamed.

Ethylene oxide emissions from medical sterilization facilities in Grand Prairie.

Styrene emissions from a bathtub manufacturing company in Lancaster.

Ethane and Methane were found in the area of gas plants in Midlothian and Wise County.

Figure 1 details the $C_{10}H_{17}$ plume encountered in Hillsboro and Figure 2 depicts a gas plume found in Wise County. The $C_{10}H_{17}$ has a very high reaction rate with the radical OH (regardless of the exact compound) which in turn leads to ozone production. The gas plume primarily consists of methane (CH_4) and ethane (C_2H_6) which can be hazardous in high enough concentrations but are not efficient ozone precursors. This is by no means a complete list but rather a brief summary of some point source measurements. More are included in the body of the report.

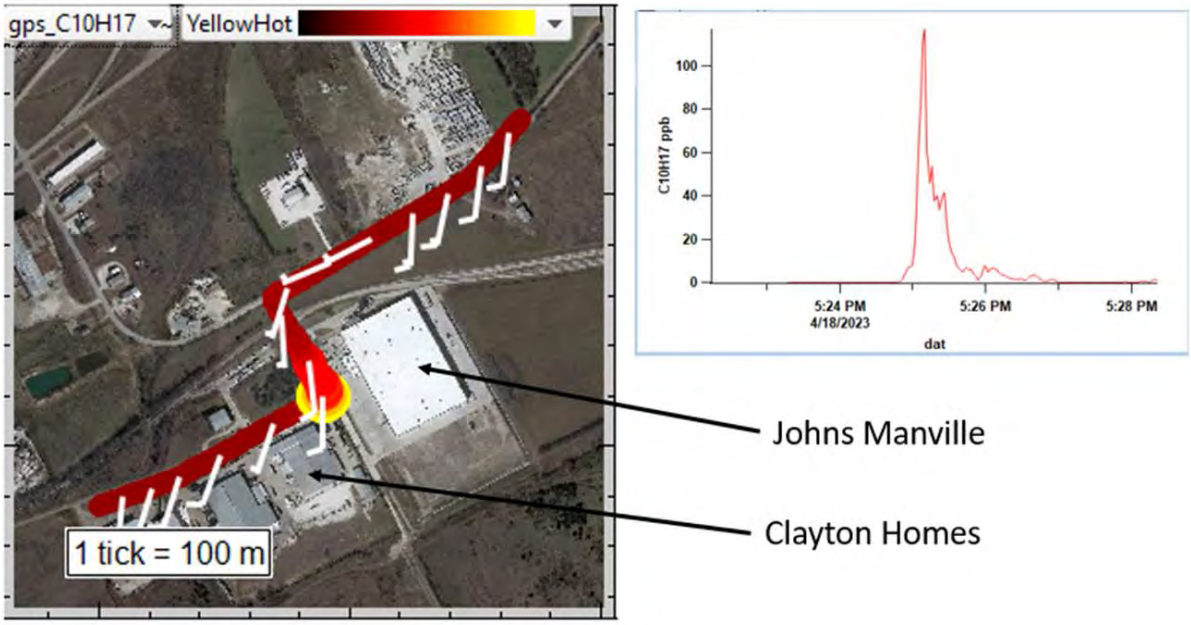

Figure 1. $C_{10}H_{17}$ plume encountered while driving the AML in Hillsboro industrial area. This plume was 97% Pinene by OH reactivity giving an [OH] reactivity of 139/second.

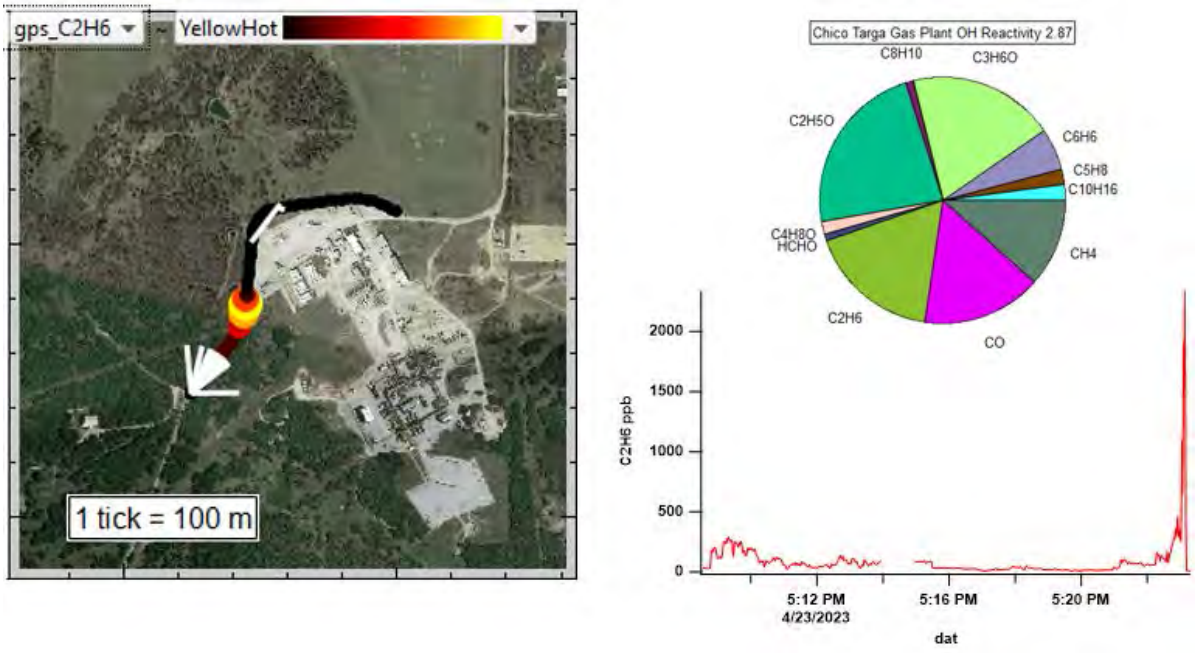

Figure 2. Plume encountered at Targa Gas Plant Chico.

The different VOC makeup among various sources leads to different OH reactivities among facilities. It is useful to have knowledge of the chemical makeup of these VOC emissions and more

thorough modeling in the future would enhance the ability to infer ozone (O_3) production related to these emissions.

For the upwind/downwind measurements Table 1 summarizes some results from these measurements. The campaign-averaged diurnal ΔO_3 was found to be 26.6 ppb. Further work with additional VOC species measured at the AML via Gas Chromatography Electron Ionization Time of Flight Mass Spectrometry (GC-EI-TOFMS) and Vocus Proton Transfer Reaction Time of Flight Mass Spectrometry (Vocus PTR-TOFMS), along with comparison of the measurements with local AutoGC measurements from the Texas Commission on Environmental Quality (TCEQ) will be useful to evaluate the relative merits of the analyses here. Modeling of this complete dataset would also be useful in interpreting the upwind/downwind evolution of the airmass.

Date	Upwind (arrival time)	Downwind (arrival time)	Max 1-min O_3 [ppb]	Max 1-hr Ox [ppb]	Ox / CO	Temp [C]	Dew Pt [C]	Solar [Ly/min]	Trimethylbenzene /Toluene
8-Apr (Sat)	McKinney (9:25 CDT)	Mansfield (16:50 CDT)	69	65.3	0.40	20.7	11.5	0.66	0.049 ± 0.003
16-Apr (Sun)	Decatur (10:37 CDT)	Palmer (15:16 CDT)	59	58.8	0.53	20.2	1.3	0.85	0.098 ± 0.006
17-Apr (Mon)	Waxahachie (11:45 CDT)	Denton (15:50 CDT)	70	**71.2**	0.41	24.9	4.7	0.77	0.068 ± 0.011
19-Apr (Wed)	Waxahachie (10:40 CDT)	Denton (16:19 CDT)	51	54.4	-	27.4	18.9	0.49	0.059 ± 0.006

Table 1. Summary of upwind-downwind experiments conducted by the Aerodyne AML during 2023 DFW AQRP study. Ox is the sum of O_3 and NO_2, solar insolation in units of Langley/minute. Temperature, dew point and solar insolation data from Meacham Field meteorological station.

For the wildfire measurement it was necessary to transport to the Wewoka Oklahoma (OK) area to measure the nearest available wildfire that could potentially at some points have impacted the DFW metro area. A biomass burning organic aerosol factor was determined from the wildfire and this was compared to a biomass burning factor from organic aerosol measurements during the

DFW metropolitan area measurements. Figure 3 shows periods in time when this factor was elevated in DFW.

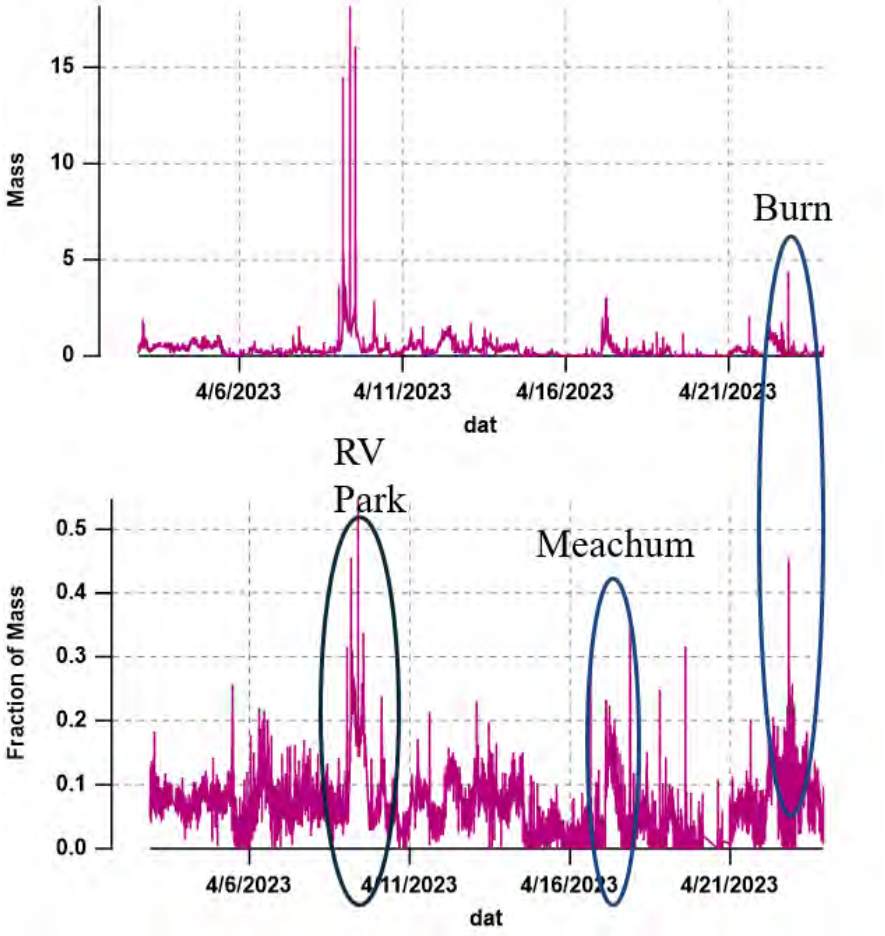

Figure 3. The biomass burning factor derived by Positive Matrix Factorization (PMF) shows over time total loading at top and fractional contribution at bottom. Note elevated factor levels on April 9 and April 17 while at the Texan Ranch RV Park and Meachum Field respectively.

Recommendations for Future Efforts:

1. Further analysis and modeling work on the point source data and upwind downwind study data specifically Positive Matrix Factorization to a larger extent of all of the gas phase and particulate phase data would yield more linkages between different data parameters in different conditions across a variety of instrumentation. This work should include comparison of these measurements with local AutoGC measurements from TCEQ. Modeling of secondary organic aerosol formation based on the measurements conducted would also help inform ozone production as well as other avenues of chemical transformation.

2. The establishment of an on-call system for measuring wildfires safely when and where they occur. It is difficult to predict far enough ahead of time given the timescales of funding when conditions will be at an optimum level for sampling wildfires and mobile measuring platforms such as the Aerodyne Mobile Laboratory are in high demand for many uses. Any means to gain flexibility in temporal sampling would be advantageous.

Table of Contents

List of Figures

List of Tables

Acronyms and Abbreviations

1,2,4-TMB: 1,2,4-Trimethylbenzene

AAE: Absorption Angstrom Exponent

AML: Aerodyne Mobile Laboratory

AMS: Aerosol Mass Spectrometer

AQRP: Air Quality Research Program

ARI: Aerodyne Research Incorporate

BB: Biomass Burning

BC^2: Black Carbon and Brown Carbon

C_2H_2: Acetylene

C_2H_4O: Acetaldehyde

C_2H_6: Ethane

CAMS: Copernicus Atmosphere Monitoring Service

CAPS-NO_2: Cavity Enhanced Phase Shift Spectrometer for NO_2

CAPS-NOx: Cavity Enhanced Phase Shift Spectrometer with Ozonator

CH_4: Methane

CO: Carbon Monoxide

CO_2: Carbon Dioxide

CPC: Condensation Particle Counter

CST: Central Standard Time

DFS: Dallas Field Study

DFW: Dallas Fort Worth

EPA: Environmental Protection Agency

EtO: Ethylene Oxide

GC: Gas Chromatography

GC-EI-TOFMS: Gas Chromatography Electron Ionization Time of Flight Mass Spectrometry

GPS: Global Positioning System

H_2O: Water Vapor

HCHO: Formaldehyde

HCN: Hydrogen Cyanide

HCOOH: Formic Acid

HGB: Houston Galveston Bay

Hz: Hertz

I-35: Interstate 35

km: kilometer

LPM: Liter Per Minute

LTO: Landing, Takeoff, Idling

m: meter

MSA: Metropolitan Statistical Area

mz: Mass to Charge Ratio

NAAQS: National Ambient Air Quality Standard

NaN: Not a Number

N_2O: Nitrous Oxide

nm: nanometer

NO: Nitric Oxide

NO2: Nitrogen Dioxide

NOx: Oxides of Nitrogen

NY: New York

O_3: Ozone

ODR: Orthoganal Distance Regression

OH: Hydroxyl Radical

OK : Oklahoma

Ox: Nitrous Dioxide plus Ozone

PI : Principal Investigator

PM : Particulate Matter

PMF: Positive Matrix Factorization

ppb: Parts per Billion

ppm: Parts per Million

ppt: Parts per Trillion

PTR-TOFMS: Proton Transfer Reaction Time of Flight Mass Spectrometry

QA: Quality Assured

RV: Recreational Vehicle

SAE: Scattering Angstrom Exponent

SAFS: San Antonio Field Study

SIP: State Implementation Plan

SP-AMS: Soot Particle Aerosol Mass Spectrometer

SS: Second Second

TCEQ: Texas Commission on Environmental Quality

TILDAS: Tunable Infrared Direct Absorption Spectrometer

TILDAS-CS: Tunable Infrared Direct Absorption Spectrometer, Compact Single-Laser

TMB:Tol: 1,2,4 Trimethylbenzene:Toluene ratio

TX: Texas

µm: micrometer

UTC: Coordínate Universal Time

UV: Ultraviolet

UZA: Ultra Zero Air

VOC: Volatile Organic Compound

Introduction

Air pollution concerns in DFW

The Dallas-Fort Worth-Arlington (DFW) Metropolitan Statistical Area (MSA) is the most populated MSA in the state of Texas and the fourth largest MSA in the United States. It is also experiencing a high rate of population and economic growth and is located along the Interstate 35 (I-35) corridor which in general is an area of rapid growth. The most recent population estimate from www.census.gov [census.gov] of the DFW MSA is 7,759,615 people with a one-year growth of 97,290 people, which equates to a growth rate of 1.02% from June 2020 to June 2021. Despite the large size and growing population, the MSA has been under-sampled with respect to air quality measurements relative to other MSAs within the state of Texas and across the country as a whole. This study provides over 50 point source measurements in this area with the purpose of beginning to understand what impact industrial sources of VOCs might have on O_3 production in the DFW metropolitan area.

Biomass burning has also recently been a matter of concern with respect to air quality in metropolitan areas in Texas. Wildfires are highly variable from year to year however the Spring is a season with relatively strong wind flow and there is seasonal crop burning which does occur at this time of year to the south on the Yucatan peninsula in Mexico [*Peppler et al.* 1999; *van der Werf et al.* 2006; *Dominguez-Martinez and Rodriguez,* 2008; *Yokelson et al.* 2009. The Aerodyne Mobile Laboratory (AML) provided a wealth of instrumentation well suited to measure biomass burning where it occurs as well as its evolution and interaction upwind, within and downwind of the DFW metropolitan area.

Project Goals

The Dallas FS field campaign was undertaken to deploy to areas of VOC emission in the DFW metropolitan area, collect measurements of VOC compounds present in ambient air directly adjacent to or near emissions sources, and gain a better understanding of the chemical speciation and magnitude of those VOC emissions. A wide variety of point sources were sampled, over 50 in number including but not limited to gas plants, cement production facilities, manufacturing businesses of various types and landfills. Additionally on 4 days upwind/downwind measurements of the DFW metropolitan area were conducted to gain a better understanding of the inflow into the DFW area and the processing and eventual outflow from the DFW area. Finally, one biomass burn was sampled and the chemical signature from that burn was used to assist in determining when biomass burning-impacted air was present in the DFW metropolitan area.

Methods

Daily Measurement Strategies

There were 3 different types of mobile measurements planned and executed during this campaign. The first type of mission involved measuring a large number of identified point sources of interest throughout the DFW metropolitan area and this occurred on most days. The second type involved going to an upwind site relative to the DFW metropolitan area, measuring for a couple of hours to establish the chemical makeup of the inflow into DFW, then transiting to a downwind site to establish the chemical makeup of that same airmass after transit through DFW and this was done on 4 days. The third mission involved going to a biomass burning site (wildfire) and measuring it. This third mission type was executed on one day. The results of all of these mission types are discussed below in the Preliminary Results Section.

Staging Base Locations

Texan Ranch RV Park

The Texan Ranch RV Park was chosen as a base of operations for the first week of the Dallas FS campaign. Originally the siting plan for the AML base of operations was to stage at the Meachum Field site detailed below for the entire period of operations but it was not ready at the campaign start date of 3 April. The Texan RV Ranch had adjacent parallel parking spots available, the necessary power and was located in an area relatively close to many of the point source locations in the Midlothian area which we desired to focus on initially. Overall, this spot worked well, there were no power issues the entire time the AML was located there. The AML was integrated there on April 3, conducting all necessary calibrations and checks prior to mobile measurements which began on April 4. Measurements were conducted at the RV ranch whenever the AML was parked there from April 3 – April 10.

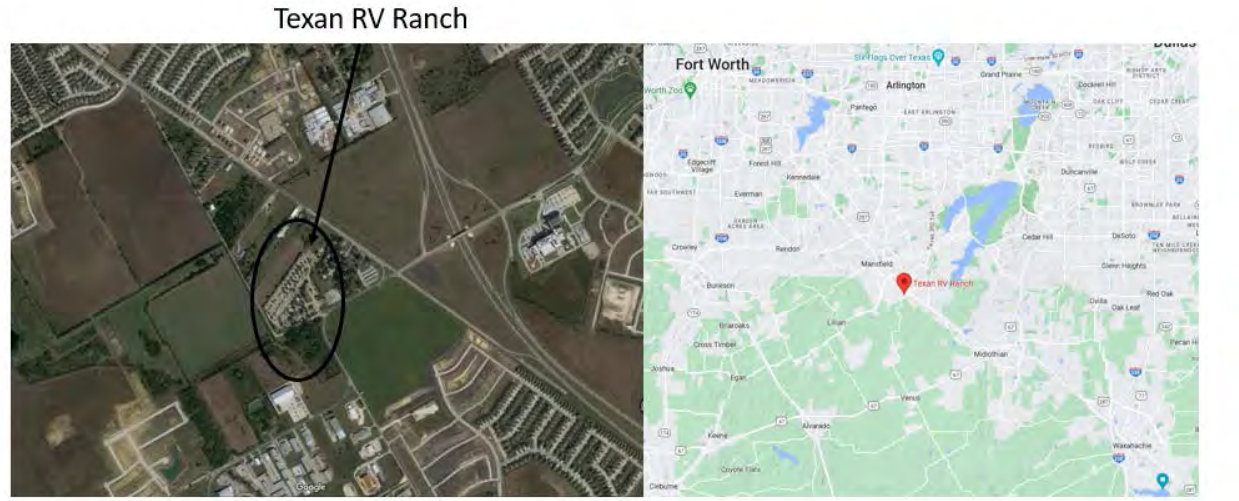

Figure 4. Map depicting location of the Texan RV Ranch RV Park in Mansfield TX.

Meachum Field

The AML transited to the Meachum Field TCEQ Northwest site on April 10th and maintained this location for the operational base through the 23rd of April. This location has several advantages including space and power available for the AML at night with much fewer interferences than the RV park was subject to. This site also had the Baylor trailer associated with AQRP Project # 22-060 conducting measurements as well as a fully outfitted TCEQ measurement station on site. This enabled co-located measurements which

are described in greater detail later. The one interference which does occasionally occur at this site is from aircraft taking off when winds are out of the north, this is also detailed later. The site is shown in Figure 5.

Figure 5. Map depicting location of field site at Meachum Field in Fort Worth TX.

Data Acquired

The Aerodyne Mobile Laboratory (AML) is a well-tested and extremely suitable measurement platform for the goals of the proposed study. Previous deployments have included the San Antonio Field Study (SAFS) [*Anderson et al.* 2019] in 2017. The AML has also conducted measurements in urban polluted areas such as Mexico City during the 2006 MaxMEX/MILAGRO campaign [*Herndon et al.*, 2008; *Wood et al.*, 2009], the 2009 Queens, NY, study [*Massoli et al.*, 2012], or for more specific sources such as aircraft emissions [*Santoni et al.*, 2011] or oil and gas extraction [*Yacovitch et al.*, 2015]. Research and commercial instruments are installed into the AML to collect data while in motion for plume characterization, area mapping or portable deployment for photochemistry and transport experiments. Real-time monitoring of both gas-phase and particulate species is the key feature of the AML.

The AML measured a number of trace gases including VOCs and particulate matter (PM) properties. Table 2 highlights the instrumentation and measured parameters on the AML. In addition to the chemical measurements described in this table, position measurements utilizing GPS and meteorological measurements of wind were key to successful mobile measurements.

Measurement	Rate	Instrument
Carbon Dioxide (CO_2)	1 s	Licor 6262
Nitrogen Dioxide (NO_2)	1 s	Cavity Enhanced Phase Shift Spectrometer for NO_2 (CAPS-NO_2)
Oxides of Nitrogen (NOx)	1 s	Cavity Enhanced Phase Shift Spectrometer with Ozonator (CAPS-NOx)
Ozone (O_3)	2 s	2B Tech Ozone Monitor
Carbon Monoxide (CO), Nitrous Oxide (N_2O), water vapor (H_2O)	1 s	Tunable Infrared Direct Absorption Spectrometer, Compact Single-Laser (TILDAS-CS): TILDAS-CS CO/N_2O analyzer.
Methane (CH_4), Ethane (C_2H_6)	1 s	TILDAS-CS CH_4/C_2H_6 analyzer.
Hydrogen Cyanide (HCN), acetylene (C_2H_2)	1 s	TILDAS-CS HCN analyzer.
Formaldehyde (HCHO), formic acid (HCOOH)	1 s	TILDAS-CS HCHO analyzer.
Black Carbon Particulate Matter (PM) (70 nm -2.5 µm)	1 s (variable)	Soot Particle Aerosol Mass Spectrometer (SP-AMS) with laser-on mode
Non-refractory PM coating on Black Carbon (70 nm – 2.5 µm)	1 s (variable)	SP-AMS with laser-on mode;
Organic, Sulfate, Nitrate, Ammonia, Chloride, metals PM (70 nm – 2.5 µm)	1 s (variable)	Aerosol Mass Spectrometer (AMS) /SP-AMS
Particle Number Density	1 s	Condensation Particle Counter (CPC)
Various Aromatics and Oxygenates such as: Benzene, Toluene, Xylene, Acetone, Acetaldehyde	1 s	Proton Transfer Reaction Mass Spectrometer (PTR-MS) VOCUS
Alkanes, Selected Alkenes and Aromatics, including alkyl nitrates	30 mins	Gas Chromatogram with Mass Spec. detection GC-EI-ToF

Table 2. Chemical parameters measured and instrumentation used for that measurement.

a. Audits of Data Quality

After the campaign, every data trace acquired was analyzed by the scientist responsible for the instrument. Each instrument's data was quality assured and output onto a 1-second time base (file names pre-pended with SS_) with the exception of the GC-EI-TOF. The GC-EI-TOF has been QA'd but due to the significantly different timing of the measurement is not on a second-second (SS) basis. Invalid data has been set to "not a number" or NaN so as not to interfere with future analysis. The following routine data quality tasks have been done:

1. calibrations were applied and data for the calibration time periods were excised,
2. clean air additions (zero air) were used to correct offsets, if needed, and data for these time periods were excised,
3. time periods of invalid data noted by experimenters during the campaign were excised.

As part of the data analysis procedure, one significant issue was discovered with a large portion of the TILDAS measurements. This problem relates to a 1 liter per minute (LPM) leak through a critical orifice discovered on April 14 and impacts CH_4, C_2H_6 and CO measurements prior to the leak fix which occurred on April 14. The upstream gas phase instruments for CO_2, Ozone and NOx/NO_2 were not affected, and neither was the dual TILDAS for ethylene oxide. The other spectrometers which measure gas and particle phase (Vocus, GC-EI-ToF, SP-AMS) were on a different inlet and were not affected.

The impact of this inlet leak is that some percentage of the measured air was originating from inside the mobile lab, as quantified by the offsets visible in the zero air overblows. This problem with the zero levels was noted early in the campaign but incorrectly diagnosed as being due to impurities in the ultra-zero air (UZA) cylinders. The total flow through the TILDAS inlet is over 10 LPM and each instrument on the inlet pulls approximately 1 LPM so this did not raise flow concerns initially.

For the affected TILDAS data prior to the 14th, the inside of the truck acts as a large air vessel with a time constant of 15-30 minutes. The truck air shows slow plumes, with fast spikes from the outdoor air on top of it. This is particularly evident for mobile methane measurements of a landfill on 4/14. We can compare the fast rise and slow decay with the inlet leak present (left, red) with the fast response measurements (right, blue) after the inlet leak was fixed.

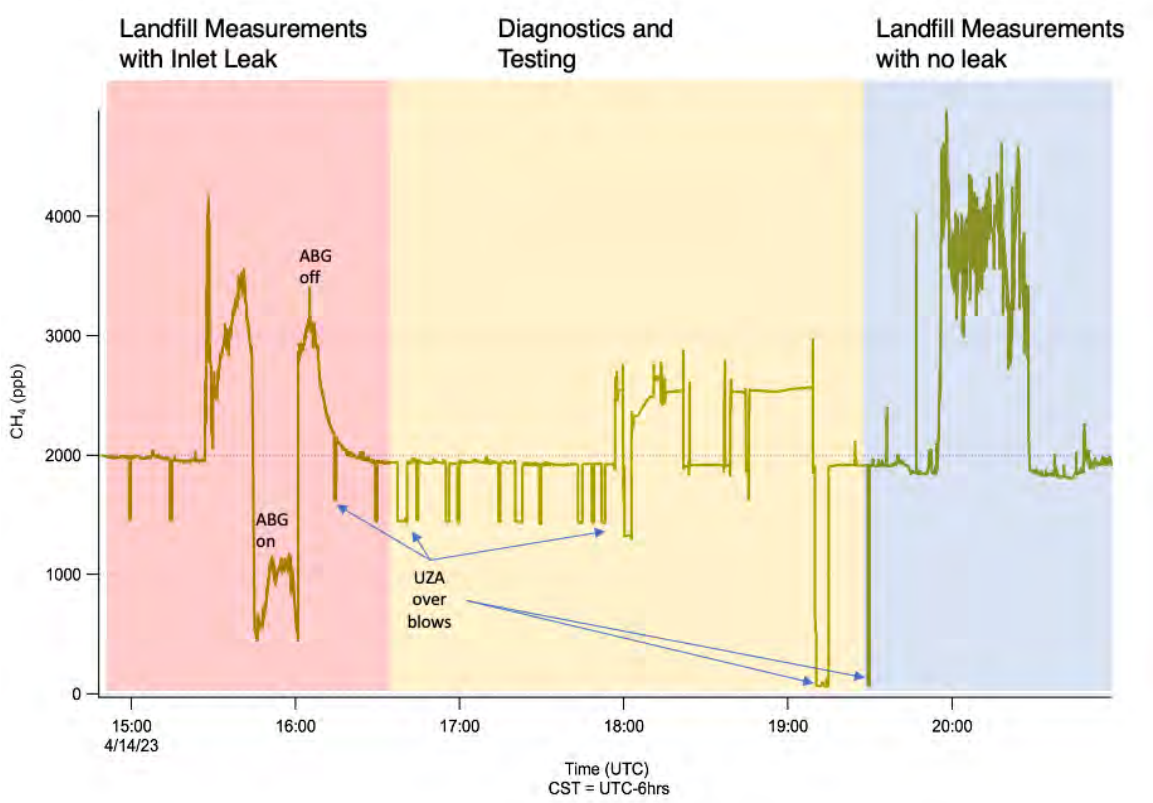

Figure 6. Methane time trace before and after inlet leak correction. Before the leak (shaded red area), the time response is slow, with a fast rise. Zero air overblows only descend from 2000 ppb to 1500 ppb. After the inlet leak is corrected (shaded blue area), the instrument zeroes completely and the time response is fast.

Several mitigation strategies were taken when this leak was discovered. 1) High-importance sites like the landfill above were re-visited after the inlet leak was corrected; 2) auxiliary measurements of CH_4, C_2H_6 and HCHO from the unaffected EtO-TILDAS were analyzed and produced as a separate data product; 3) stationary data prior to April 14 was kept in the data stream, with the assumption that ambient concentration measurements should be correct, as long as the time constant is considered.

Furthermore, the data quality officer, Dr. Ed Fortner, has performed a data quality audit. This audit was done by loading and graphing final 1-second data files from each scientist (or start-stop files for the gas chromatograph). Ten percent of the data has been thoroughly examined and where corrections have been such as in the case of the critical orifice leak referred to above that data has been corrected and found to be acceptable or discarded. In cases where data has been discarded auxiliary measurements from the EtO-TILDAS instrument are used.

Preliminary Results

Point Source Measurements

One of the primary goals of the Dallas FS was to measure a variety of point sources in the DFW metropolitan area with an emphasis on ozone precursor measurements. Point source measurements were carried out on 14 days at a variety of locations within the DFW area. The publicly available site level summary emissions inventory data from 2021 https://www.tceq.texas.gov/airquality/point-source-

ei/psei.html was used as a guide for locations to examine. Over 50 industrial facility point sources of interest were measured with over 30 facilities identified as emitting measurable plumes of gas phase and particle phase compounds above ambient background levels. A table depicting locations visited with the AML is shown in Table 3. These locations are sorted by VOC ton per year emission and locations with emissions detectable above ambient background levels are colored in orange.

ACCOUN	RN	COMPAN	SITE	COUNTY	REGION	SIC	DESCRIP	RTING	CO TPY	NOX TPY	Pb TPY	PM10 TPY	M2.5 TP	SO2 TPY	VOC TPY
ED0168P	RN10021	DARTCO C	DARTCO C	ELLIS	4	3089	PLASTICS	2021	25.19	11.23	0.0001	2.327	2.327	0.18	611.368
TA0157I	RN10250	GENERAL	ARLINGTC	TARRANT	4	3711	MOTOR VI	2021	39.5258	53.6743		6.6924	6.5323	0.2498	418.711
ED0011D	RN10021	CHAPARR	CHAPARR	ELLIS	4	3312	BLAST FUI	2021	1535.71	411.191	0.4274	148.02	127.628	315.138	332.102
JHA012L	RN10492	ETC TEXAS	GODLEY P	JOHNSON	4	1321	NATURAL	2021	110.392	48.2571		9.446	9.446	4.297	216.931
ED0099J	RN10021	HOLCIM L	MIDLOTH	ELLIS	4	3241	CEMENT, I	2021	2894.62	1249.65	0.0121	284.294	165.813	1898.78	188.066
TA0156K	RN10021	LOCKHEEI	US AIR FO	TARRANT	4	3721	AIRCRAFT	2021	3.2714	9.231	0	11.2886	11.2636	2.1778	139.443
JH0025O	RN10021	JOHNS MA	JOHNS MA	JOHNSON	4	3296	MINERAL	2021	362.182	42.4523	0.0002	183.539	179.76	21.5605	135.506
NB0089J	RN10022	PACTIV LL	PACTIV CC	NAVARRO	4	3086	PLASTICS,	2021	6.0583	7.2465	0	22.242	21.5498	0.1241	104.1
ED0051O	RN10022	OWENS CI	WAXAHAC	ELLIS	4	3296	MINERAL	2021	164.975	73.4993	0.0001	259.861	217.117	14.4768	84.2756
WN0021(	RN10022	ENLINK M	BRIDGEPC	WISE	4	1321	NATURAL	2021	220.744	299.743	0	19.7529	19.7529	1.0123	71.267
ED0013W	RN10253	PRAXIS CC	KORAL INI	ELLIS	4	3088	PLASTICS,	2021	0.2182	0.2598	0	0.0519	0.0277	0.0015	70.6563
TA0236L	RN10022	BALL MET	BALL MET	TARRANT	4	3411	METAL CA	2021	5.9798	7.1186		0.5727	0.5517	0.0429	69.6195
DF0051J	RN10021	PACCAR IN	PETERBILT	DENTON	4	3711	MOTOR VI	2021	10.7553	12.3585	0	10.5272	0.3568	0.085	64.704
DB0447B	RN10068	HENSLEY I	DALLAS PI	DALLAS	4	3325	STEEL FOU	2021	67.2284	11.4075		7.265	7.1506	3.0224	63.4473
TA0054T	RN10022	BELL TEXT	PLANT 1	TARRANT	4	3721	AIRCRAFT	2021	10.8087	12.1485	0	4.9492	0.9694	0.1013	60.8695
DB1276U	RN10021	TEKNI-PLE	DOLCO PA	DALLAS	4	5169	CHEMICAI	2021	0.5185	0.6173		0.049	0.049	0.0037	57.2995
DB0820B	RN10250	TEXAS INS	CENTRAL I	DALLAS	4	3674	SEMICONI	2021	44.1592	54.8238		10.2643	5.7823	6.2977	57.1955
WN0005E	RN10023	TARGA MI	DYNEGY C	WISE	4	1321	NATURAL	2021	41.91	100.12		5.58	5.58	35.1039	54.95
DB3613K	RN10230	WESTERN	CEDAR HII	DALLAS	4	2434	WOOD KI	2021	0.0824	0.098	0	0.0321	0.0321	0.0006	54.6498
DB0155R	RN10066	TAMKO BI	DALLAS PI	DALLAS	4	2952	ASPHALT I	2021	31.2668	7.4049	0	13.2361	9.8371	29.3555	53.9459
PCA008H	RN10501	BKV MIDS	WEST WA	PARKER	4	1311	CRUDE PE	2021	11.0563	28.1575		0.0917	0.0917	0.1701	52.6513
DB0588F	RN10024	MAGELLA	DALLAS TE	DALLAS	4	4226	SPECIAL V	2021	0	2.56	0	0	0	6.4	52.106
DB0795V	RN10051	MOTIVA E	DALLAS TE	DALLAS	4	5171	PETROLEU	2021	2.7983	1.3916		0.0863	0.0751	0.0012	51.6126
JH0376F	RN10077	TECHNICA	TECHNICA	JOHNSON	4	2899	CHEMICAI	2021	0.035	0.0028	0	0.035	0.035	0.0028	45.1843
DBA035J	RN11027	E R CARPE	EPS INSUL	DALLAS	4	3086	PLASTICS,	2021	1.4663	0.8728	0	0.1327	0.1327	0.0105	45.0617
DB5077A	RN10075	CITY OF D	MCCOMM	DALLAS	4	4953	REFUSE SY	2021	1.927	8.82	0	82.575	50.583	0.586	43.005
TA1222P	RN10249	FLINT HILI	FORT WOI	TARRANT	4	5171	PETROLEU	2021	1.7708	0.731		0.0395	0.0058	0.0002	39.9604
ED0066B	RN10021	TXI OPERA	MIDLOTH	ELLIS	4	3241	CEMENT, I	2021	510.11	1495.19	0.0074	207.908	95.6833	669.6	39.6424
TAA045S	RN10300	BIMBO BA	TIA ROSA (	TARRANT	4	2051	BREAD, CA	2021	0.6127	0.7294	0	0.1269	0.1269	0.0044	39.555
CP0396W	RN10021	ENCORE W	MCKINNE	COLLIN	4	3351	COPPER R	2021	172.602	15.0729	0.0312	12.1931	11.3635	0.1793	38.4687
DF0089H	RN10261	TETRA PAI	MATERIAL	DENTON	4	2656	SANITARY	2021	0.934	1.111	0	0.463	0.463	0.006	38.212
TA0172M	RN10021	FORT DEA	FORT WOI	TARRANT	4	2752	COMMERC	2021	0.09	0.11	0	0.01	0.01	0.001	37.2176
TA0235N	RN10264	MOLSON (	FORT WOI	TARRANT	4	2082	MALT BEV	2021	19.433	8.9051	0	1.8611	1.8546	0.1549	36.8391
DB0976P	RN10021	AQUATIC (	AQUATIC	DALLAS	4	3088	PLASTICS,	2021	0.02	0.02		0.002	0.002	0.0002	36.7129
PC0011B	RN10218	MAGELLA	ALEDO PR	PARKER	4	4613	REFINED F	2021	3.7083	1.8575	0	0.0018	0.0018	0.0034	36.3491
TAA062J	RN10060	PARKER-H	MANSFIEL	TARRANT	4	3052	RUBBER &	2021	0	0	0	0	0	0	35.3626
DF0223E	RN10054	WASTE MA	DFW RECY	DENTON	4	4953	REFUSE SY	2021	269.86	79.2	0	25.15	20.48	45.59	35.21
JHA004D	RN10437	ENERGY TI	CLEBURNI	JOHNSON	4	4922	NATURAL	2021	19.2738	29.8051		3.5533	3.5533	0.202	33.1347
TA0051C	RN10221	BELL TEXT	PLANT 5A	TARRANT	4	3721	AIRCRAFT	2021	5.6046	4.0896	0	4.31	4.31	0.0319	33.0545
DB4237J	RN10200	CITY OF IR	HUNTER F	DALLAS	4	4953	REFUSE SY	2021	0.7201	0.7201	0	8.4701	1.45	0.0001	32.39
DBA014N	RN10507	OVERWRA	OVERWRA	DALLAS	4	2759	COMMERC	2021	1.06	1.25		0.092	0.092	0.0066	32.293
DB0408L	RN10164	PPG ARCH	PAINT MF	DALLAS	4	2851	PAINTS AN	2021	0.2118	0.252	0	1.1597	1.1597	0.0016	31.7187
TA0142V	RN10022	US VENTU	US OIL FO	TARRANT	4	5171	PETROLEU	2021	0.0555	0.034				0.0016	30.4521
DB0969M	RN10055	RMAX INC	FOAM BO	DALLAS	4	3086	PLASTICS,	2021	0	0	0	0	0	0	27.21
TAA001A	RN10321	BIMBO BA	BIMBO BA	TARRANT	4	2051	BREAD, CA	2021	1.2892	1.5347	0	0.2201	0.2201	0.0092	26.8294
DB0135A	RN10056	HATCO IN	HATCO	DALLAS	4	2353	HATS, CAF	2021	0.754	0.898	0	0.429	0.068	0.0052	24.8401
ED0034O	RN10022	ASH GROV	MIDLOTH	ELLIS	4	3241	CEMENT, I	2021	149.4	531.154	0.0078	79.7479	71.112	7.6331	17.8399
ED0332D	RN10259	MIDLOTH	MIDLOTH	ELLIS	4	4911	ELECTRIC	2021	848.762	241.956	0	112.247	112.247	9.5874	15.7371
JH0398S	RN10082	TEXAS REC	TURKEY CI	JOHNSON	4	4953	REFUSE SY	2021	6.9504	1.2806	0	22.475	13.072	2.45	13.6438
ED0319S	RN10055	QUALICO	STRUCTUI	ELLIS	4	3441	FABRICAT	2021	0	0	0	0.0048	0.0048	0	10.602
ED0152H	RN10146	MARTECH	MARTECH	ELLIS	4	3299	NONMETA	2021	0	0	0	0.52	0.52	0	10.052
EDA010J	RN11073	BOMBARI	RED OAK F	ELLIS	4	3721	AIRCRAFT	2021	0	0	0	0	0	0	10.0194
ED0146C	RN10068	LIFOAM IN	LIFOAM IN	ELLIS	4	3086	PLASTICS,	2021	1.964	2.33	0	0.177	0.177	0.014	5.884

Table 3. Partial list of locations sampled by the AML. Locations depicted in orange had measurable plumes sampled above background levels while those depicted in yellow did not.

Every plume sampled is an interesting story in its own right and it would be beyond the scope of this report to discuss every plume in detail. There are certain plumes of interest which are discussed in greater detail in the following section because they help to emphasize features of importance relative to the overall point source measurement mission.

Owens Corning/DARTCO Waxahachie Point Source Measurements

A sequence of measurements conducted in the Waxahachie area is interesting to consider. There are multiple facilities in this area and there are roads present to sample on, however the road structure is not grid-like and under many different wind vectors it is difficult to isolate just one potential source. On April 4 while driving in the Waxahachie area, a clear plume was encountered immediately downwind of the Owens Corning facility. Winds were strong out of the south on this day. VOCs detected by the Vocus instrument showed immediate enhancement (Figure 7). It should also be noted that Dartco Container Corporation is further upwind of this plume, so it is hard to rule out any impact from the Dartco facility.

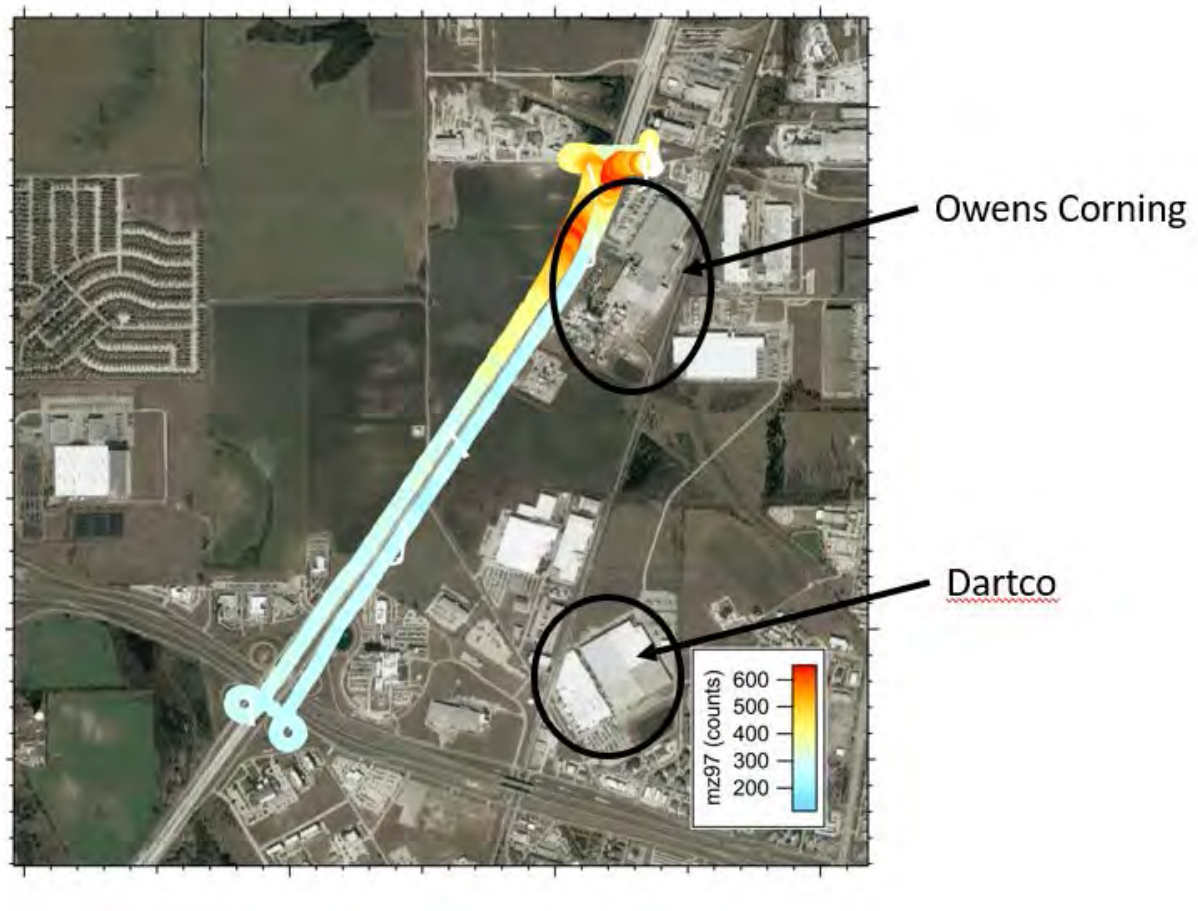

Figure 7. The route of the AML is depicted by the colored trace. The trace is colored by mz 97 counts from the Vocus typically attributed to vinyl chloride.

The next day April 5th winds shifted to being out of the northwest and while this wind does not work well for sampling Owens Corning, it is useful for sampling Dartco. Figure 8 depicts measurements of a plume immediately downwind of the Dartco facility. The AML was able to park in this plume enabling GC-EI-ToF measurements of this plume in addition to the typical one second measurements of gas phase and particle phase species.

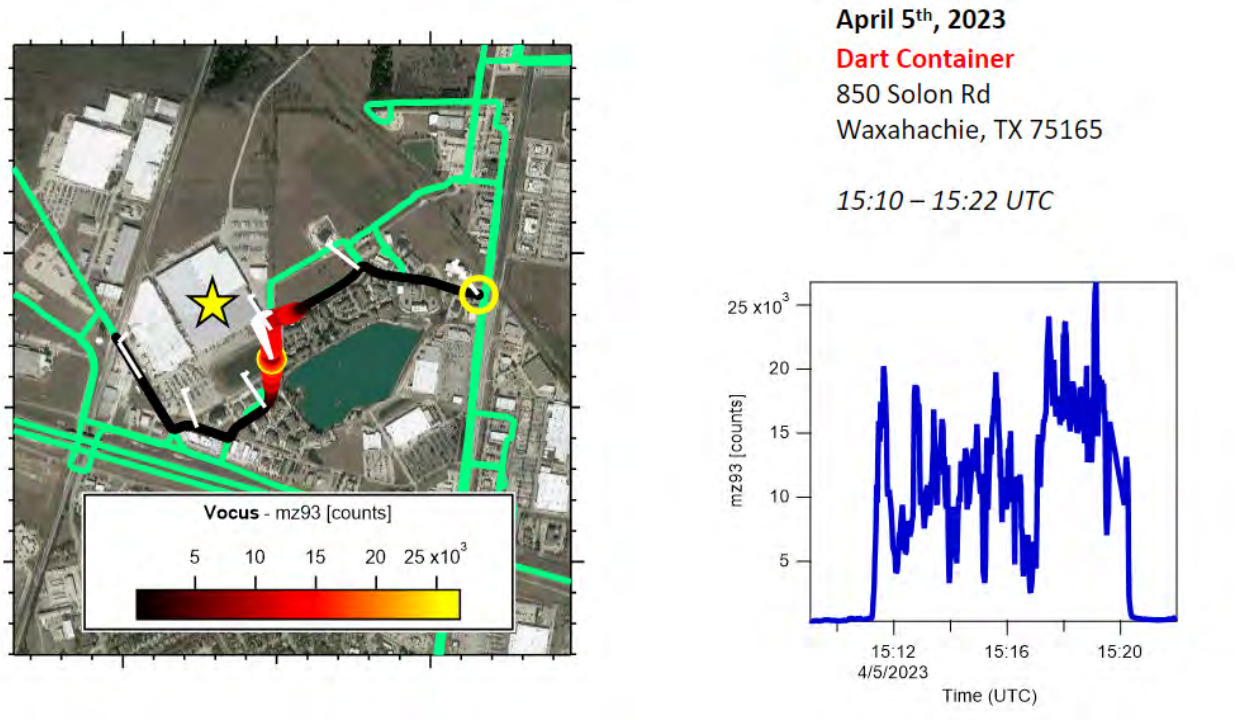

Figure 8. The route of the AML is depicted at left colored by the mz 93 (toluene) intensity as measured by Vocus and the time series of mz 93 (toluene) is depicted at right.

Finally on April 10th measurements were conducted in the Waxahachie area with an east wind. This wind worked well for measuring both Owens Corning and Dartco without their respective plumes overlapping each other (Figure 9).

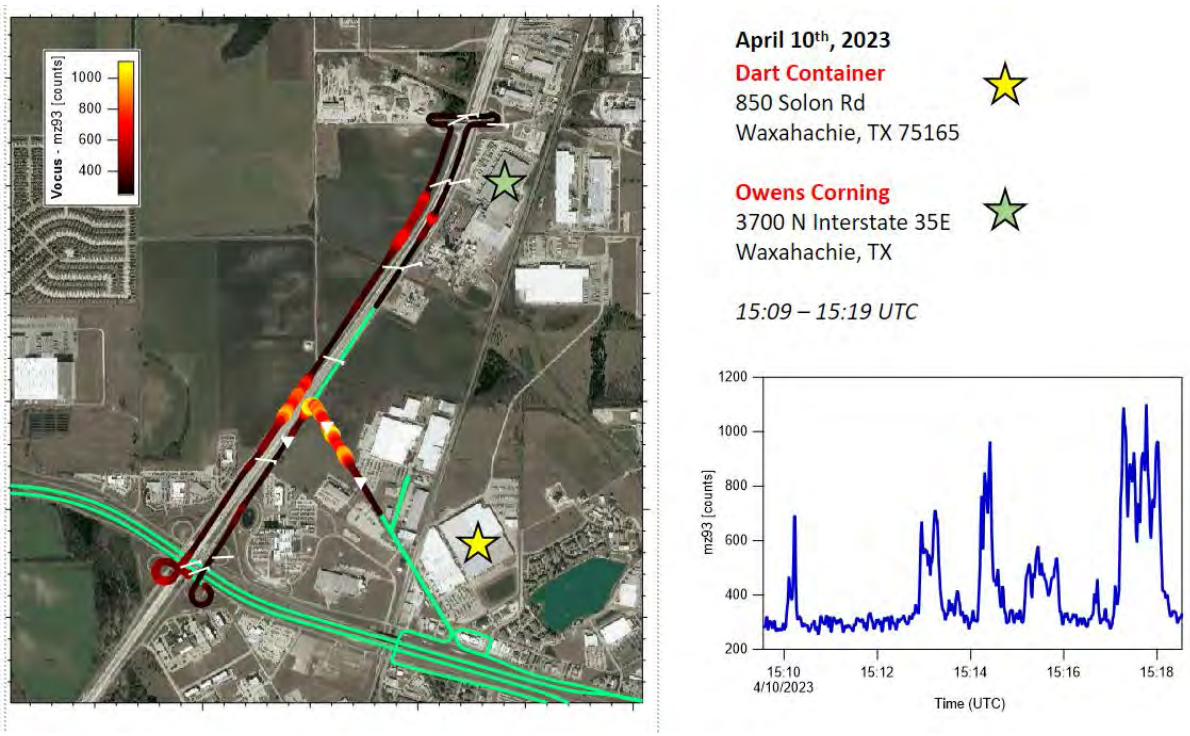

Figure 9; The route of the AML is depicted at left colored by the mz 93 (toluene) intensity as measured by Vocus and the time series of mz 93 (toluene) is depicted at right

Now that the plumes have been differentiated by source, it is possible to examine their chemical structure separately. Using the measured concentration in ppb of the various gas phase components present in the plume and using *k*[OH] reaction rates published in [*Manion et al.*, 2015][*Gilman et al.*, 2015] we can determine respective [OH]/second reactivity overall and by individual species. Figure 10 depicts the OH reactivities apportioned by species as a percentage of the whole for both the Owens Corning and DARTCO plumes. The Owens Corning plume OH reactivity is dominated by Acetaldehyde, CO, CH_4 and Formaldehyde while the DARTCO plume is dominated by Xylenes and C9 species. It should be noted that while the overall OH reactivity as measured is higher in the DARTCO plume it is difficult to account for dilution making the overall percentages of reactivity by species the more useful measured parameter.

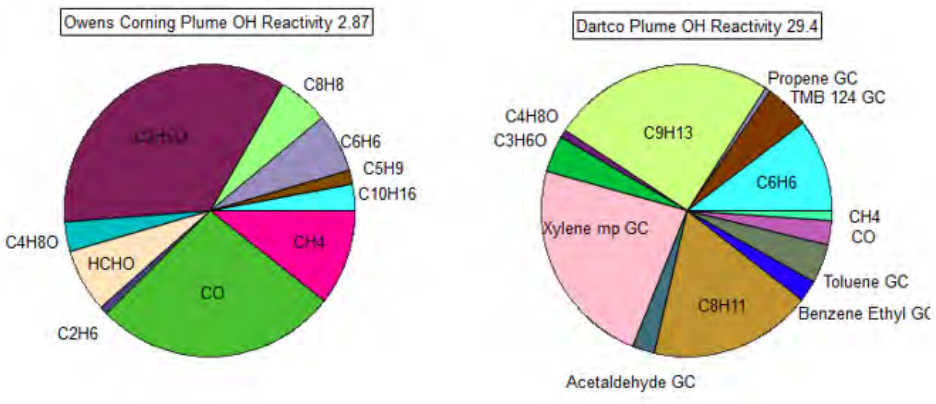

Figure 10. OH reactivities determined for the Owens Corning and Dartco plumes.

Hillsboro Clayton Homes Plume

On April 18th the AML drove south to Hillsboro TX to measure around the new Johns Manville facility constructed in 2022. In the area an intense plume of $C_{10}H_{17}$ (Pinenes and other VOCs) was encountered (Figure 11). Due to the relatively strong south wind on that day and noting that the signal was not encountered upwind of Johns Manville but instead upwind of Clayton Homes we believe Clayton Homes is the most likely emitting facility. This plume was almost entirely $C_{10}H_{17}$. By OH reactivity, it was 97% of total OH reactivity in the plume and the overall OH reactivity was 139/second, the highest measured in this campaign to date.

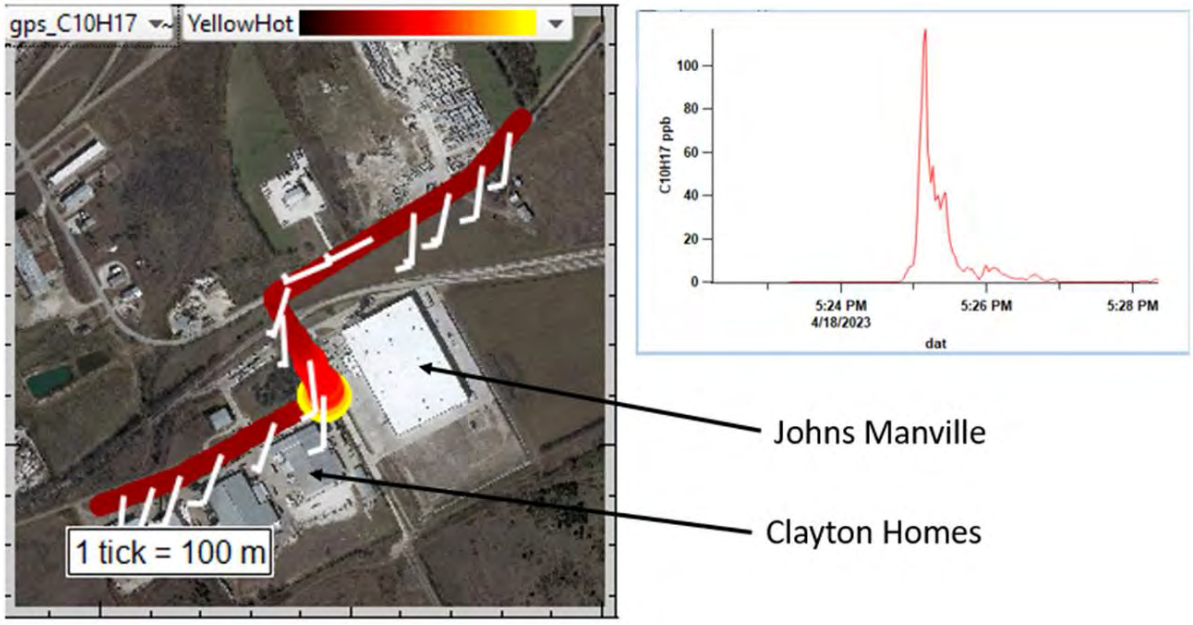

Figure 11; $C_{10}H_{17}$ plume encountered while driving the AML in Hillsboro industrial area.

Aquatic Lancaster TX

On April 21st the AML drove to the Lancaster area and sampled on the street outside of Aquatic (bath manufacturer). Traffic conditions, winds and available parking allowed the AML to get a very clear sample of the building with minimal interferences (Figure 12). A GC sample which lasts 10 minutes was taken during this period. Styrene was being emitted at this facility along with C_3H_6O which may be either acetone or propanal. The GC was sampling acetone and by subtracting the GC derived acetone from the overall C_3H_6O signal we come up with approximately 30% of the overall signal at C_3H_6O being attributed to

propanal. Propanal has a significantly higher *k*[OH] than acetone (20 to .19) so this is a potential source for error, however the bulk of the signal from the plume is at styrene which is measured with both GC and Vocus and that measurement is consistent between the Vocus and the GC-EI-ToF. The overall OH reactivity was 25.7.

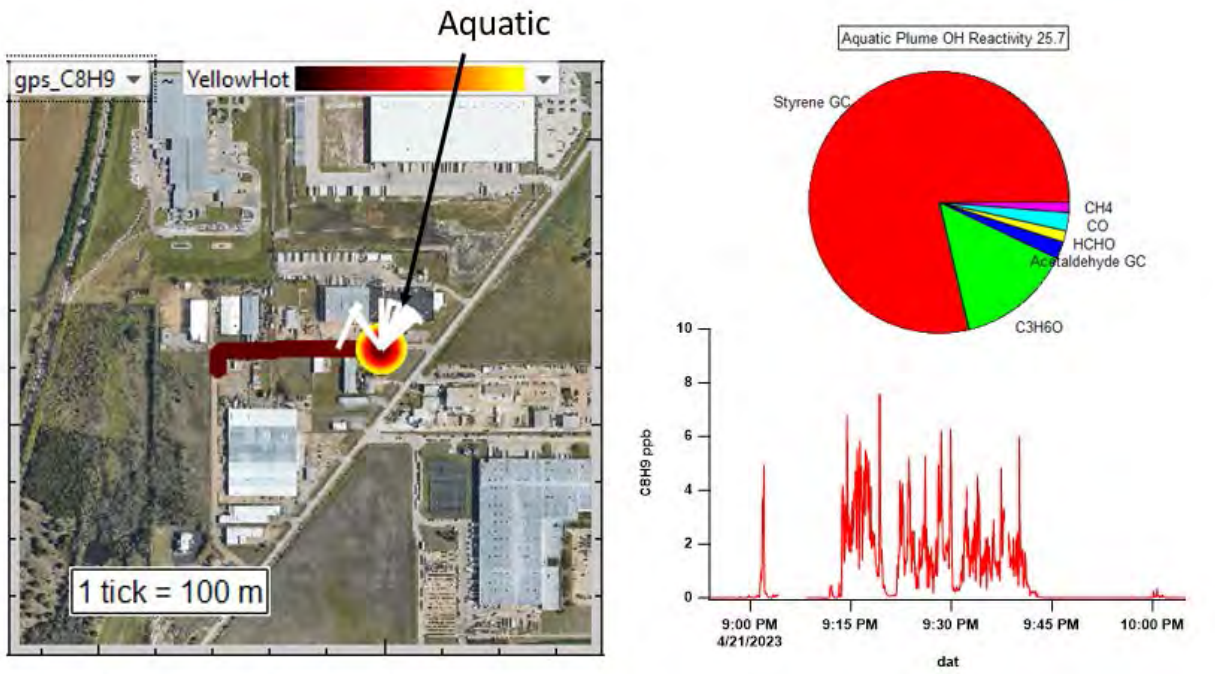

Figure 12. Styrene plume encountered outside Aquatic in Lancaster TX.

Chico Targa Gas Plant

On April 23rd the AML conducted transects in the natural gas processing regions in Wise County. The Chico Targa Gas Plant had a very elevated ethane (C_2H_6) signal. This plume was a factor of 5 higher in signal relative to any other C_2H_6 plume encountered during the Dallas FS. This was a very clear signal on a lightly travelled road with a consistent northeast wind (figure 13). Despite the high C_2H_6 signal overall OH reactivity was somewhat muted at 2.87. C_2H_6, C_2H_4O, CH_4, C_3H_6O and CO were all significant portions of the total OH reactivity.

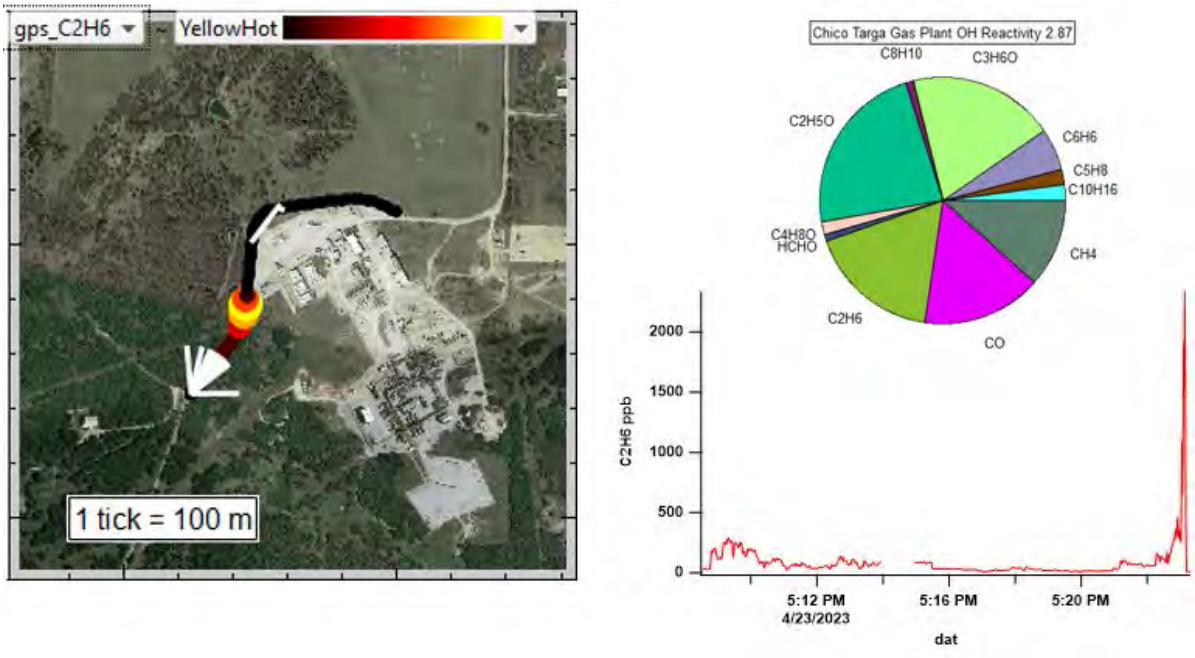

Figure 13. Plume encountered at Targa Gas Plant Chico TX.

Ethylene Oxide (EtO) Measurements

Between April 3nd and April 24th, the Aerodyne Mobile Laboratory sampled numerous known industrial sources of VOCs around the Dallas-Fort Worth-Arlington area. Data shown in Figure 14 contains both in-motion (during the day) and stationary periods (at night) between April 15th and April 24th. Noise precision at 1 Hz is 57.5 ppt, averaging down to 28.5 ppt in 100 seconds. No notable plumes of EtO were observed during this time period. Spectral backgrounding using ultra zero air occurred every 20 minutes (for a 1 minute duration), which reduces the optimal precision achievable with more frequent zeroing (typically every 5 minutes).

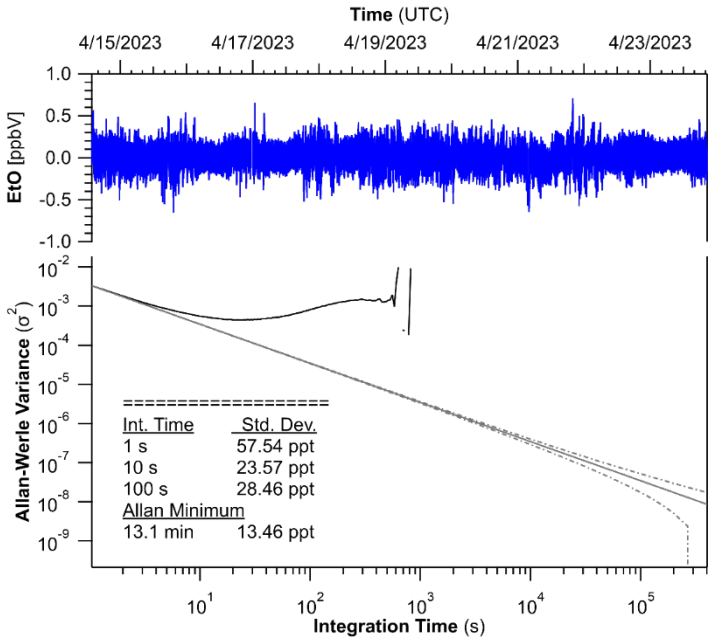

Figure 14. Allan-Werle Variance plot of ethylene oxide data measured by an EtO-TILDAS (413 m cell) while sampling emission sources around Dallas-Fort Worth-Arlington between April 14 and April 23.

While stationary, noise precision is reduced only slightly (54 ppt at 1 Hz) despite the potential for motion-related sensitivity with the finely tuned alignment of the 413 m cell (figure 15). Data was collected during an hour-long break in Grand Prairie, Texas at a shopping area approximately 4 km away from two facilities using EtO for sterilization processes.

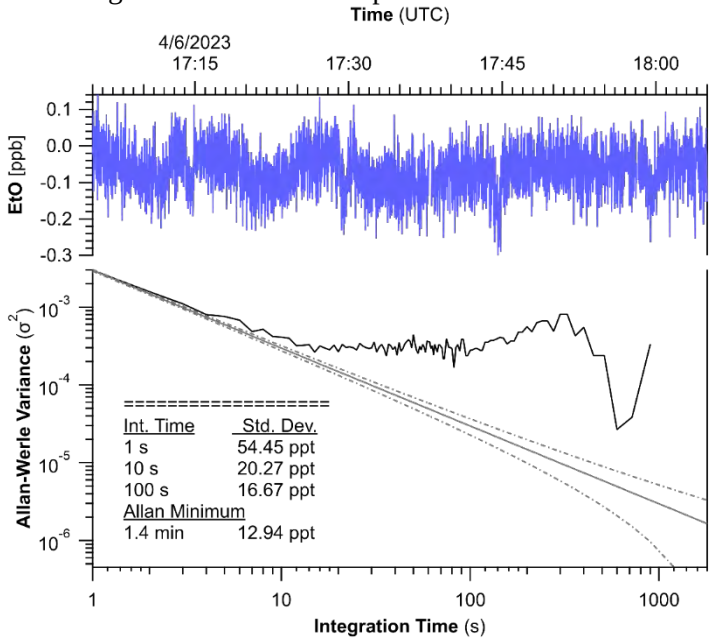

Figure 15. Allan-Werle Variance plot of ethylene oxide data measured by an EtO-TILDAS (413 m cell) while stationary in Grand Prairie, Texas on April 6, 2023.

During a 5-minute period, while driving on the northwest border of the Great Southwest Industrial District in Grand Prairie, Texas, approximately 0.5 – 1.5 km away from the two facilities employing EtO, the EtO-TILDAS experienced noise precision of 60 ppt at 1 Hz. This background data was upwind of the facilities using EtO and occurred between downwind measurement periods.

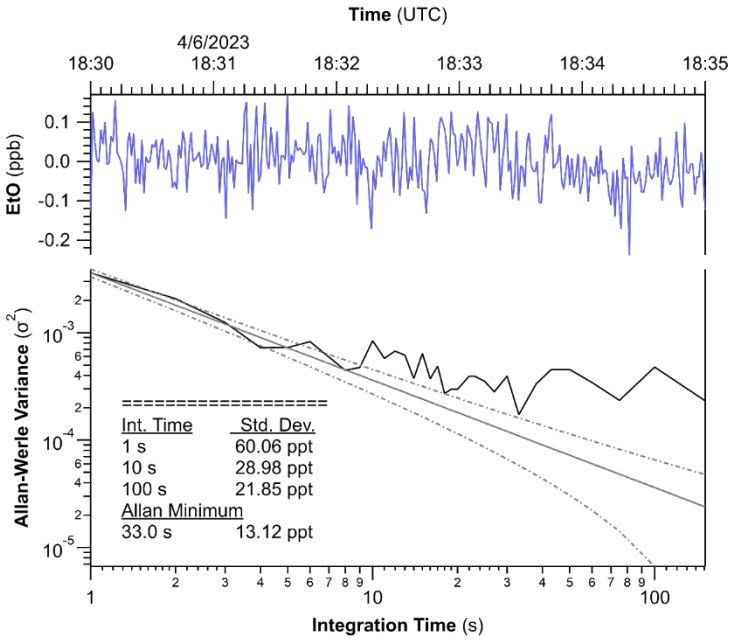

Figure 16. Allan-Werle Variance plot of ethylene oxide data measured by an EtO-TILDAS (413 m cell) while in-motion in Grand Prairie, Texas on April 6, 2023.

The two facilities using EtO in the Great Southwest Industrial District of Grand Prairie, Texas, are Sterigenics U.S. LLC (1302 Avenue T) and Isomedix Operations, Inc. (1175 Isuzu Pkwy), per the EPA (as of April 24, 2023). During mobile surveys downwind (NW) of Sterigenics (between 18:18 – 18:29 UTC and 18:42 – 18:44 UTC) peak concentrations between 7 – 12 ppb were observed as broad plumes (at 350 m away). Lack of road availability limited proximate downwind access to Steris, but multiple transects at 800 m away still encountered enhanced concentrations of EtO (~ 1 ppb) between 18:37 and 18:40 UTC.

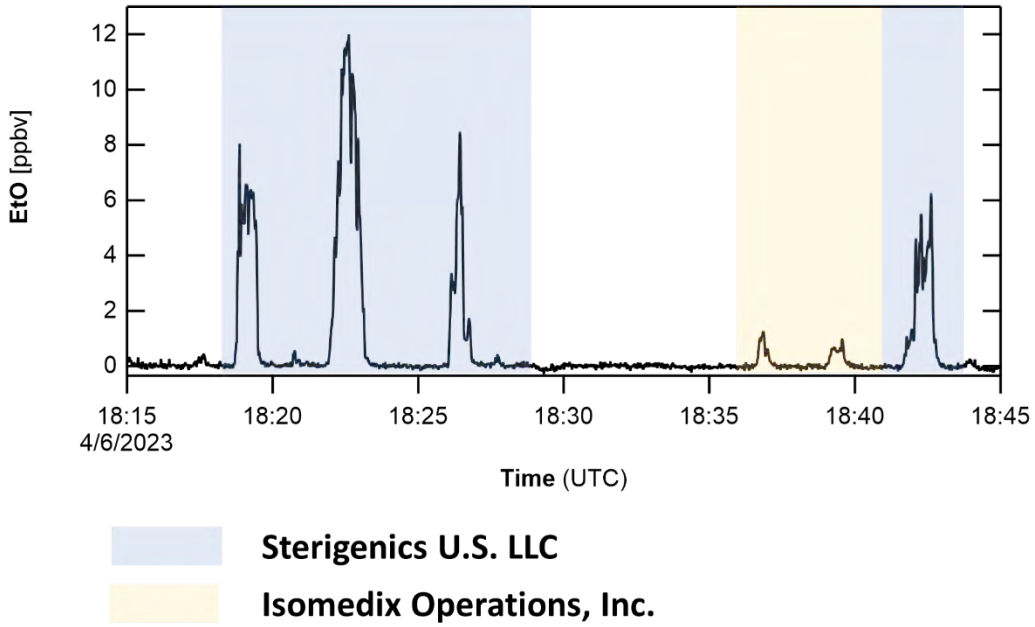

Figure 17. Time series of ethylene oxide concentrations observed during mobile sampling between 18:00 – 19:00 UTC in the Great Southwest Industrial District of Grand Prairie, Texas, on April 6, 2023. Blue areas indicate times downwind of Sterigenics U.S. LLC, while yellow areas indicate times downwind of Isomedix Operations, Inc.

A concentration map of the time series shown in Figure 17 is colored and sized by EtO concentration between 0 – 10 ppb (Figure 18). As previously noted, the dominant wind direction during this time period was from the northeast (as indicated by the white arrow). Visually, it is clear to see the emissions downwind of Sterigenics that do not appear immediately upwind of the facility. Similarly, subtle concentration rises downwind of Isomedix (at significant distance) do not appear upwind.

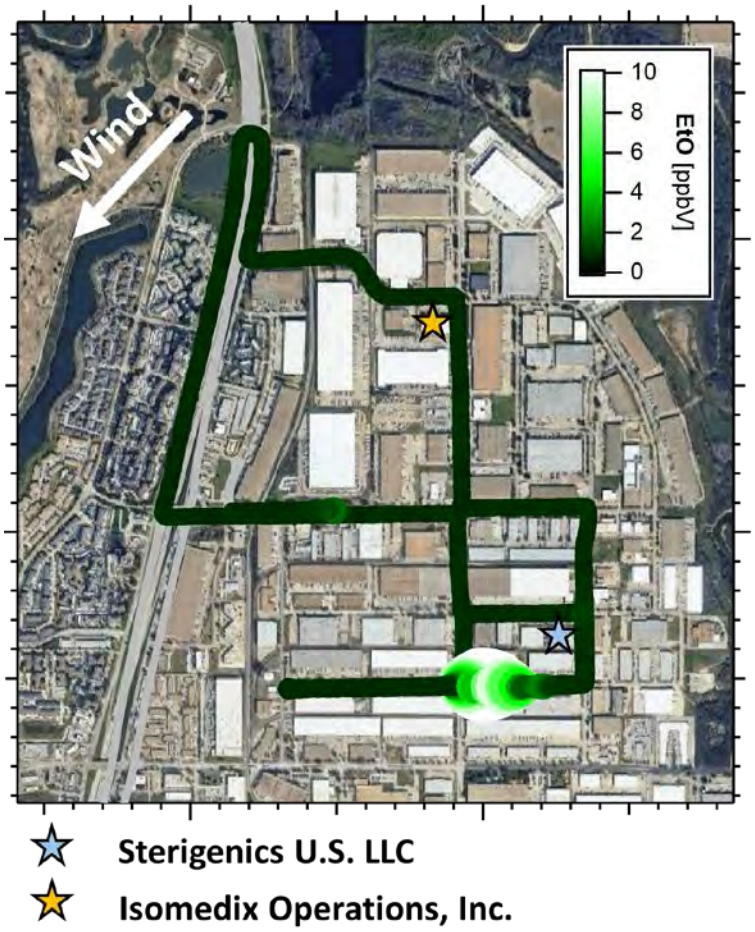

Figure 18. Mapping of ethylene oxide concentrations observed during mobile sampling between 18:15 – 18:45 UTC in the Great Southwest Industrial District of Grand Prairie, Texas, on April 6, 2023.

Upwind – downwind experiments during DFW AQRP study

On Nov. 16, 2017, EPA designated a majority of Texas as attainment/unclassifiable for the 2015 eight-hour ozone NAAQS (0.070 ppm). On June 4, 2018, EPA published final designations for the remaining areas. Consistent with state designation recommendations, EPA finalized nonattainment designations for a nine-county DFW marginal nonattainment area (Collin, Dallas, Denton, Ellis, Johnson, Kaufman, Parker, Tarrant, and Wise counties) and a six-county HGB marginal nonattainment area (Brazoria, Chambers, Fort Bend, Galveston, Harris, and Montgomery counties).

The attainment deadline for the DFW and HGB marginal nonattainment areas was Aug. 3, 2021, which was not met. The attainment deadline for the Bexar County marginal nonattainment area was Sept. 24, 2021, which was not met. On April 13, 2022, EPA proposed to reclassify the DFW, HGB, and Bexar County areas to moderate and disapprove the Bexar County 179B Demonstration SIP Revision. EPA is proposing

Jan. 1, 2023, as the deadline for TCEQ to submit federally required moderate classification SIP revisions. Attainment for all three areas would be required by the end of 2023 to meet the attainment dates of Aug. 3, 2024, for the DFW and HGB areas and Sept. 24, 2024, for the Bexar County area.

Overview of ozone mixing ratio in DFW during campaign.

Ozone mixing ratios in the DFW region typically peak between May and October but can still show 8-hour averaged ozone maxima above 60 ppb during April, the time of this study. Maximum 8-hour averaged daily ozone mixing ratios from two TCEQ air monitoring sites are shown in Figure 19 for 2022.

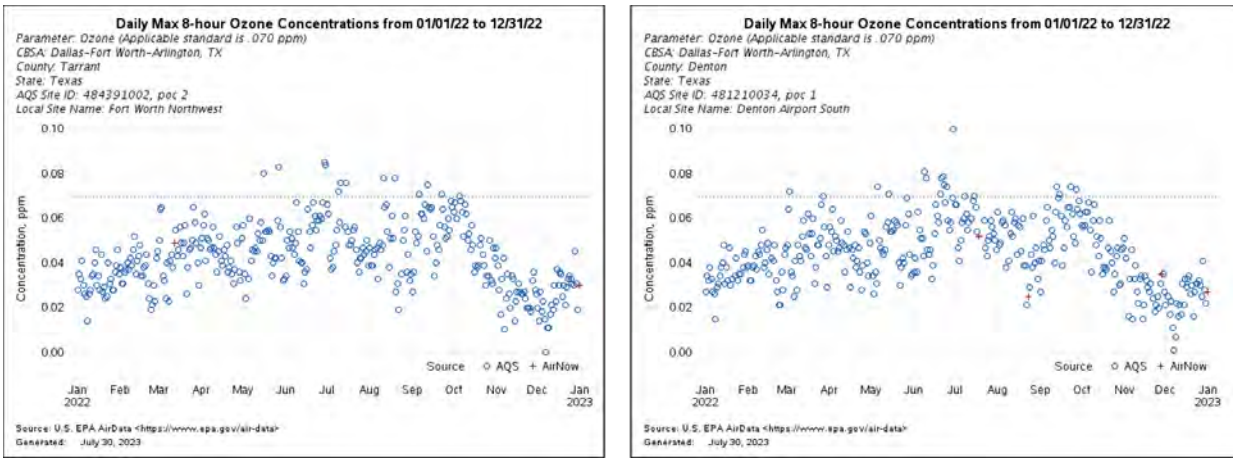

Figure 19. Air quality data for 2022 for two TCEQ monitoring stations [Fort Worth Northwest, Station ID 484391002 and Denton Airport South, Station ID 481210034], showing daily 8-hr maximum ozone in ppm. Points above the dashed line represent exceedances of the 2015 NAAQS 8-hr ozone standard.

During the 2023 DFW AQRP study, ozone monitors throughout the region showed no 8-hour exceedances and even the 1-hour daily maximum values observed were below 70 ppb (Figure 20).

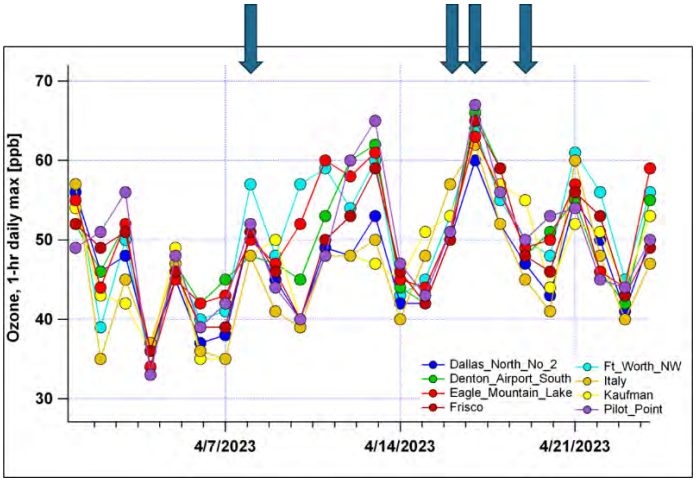

Figure 30. Daily maximum ozone in ppb, 1-hr average, from eight TCEQ monitoring sites around the DFW region. Arrows indicate days where ARI conducted upwind / downwind studies (8-Apr, 16-Apr, 17-Apr, 19-Apr). Data from of www.tceq.texas.gov website.

As part of the instrument package on the ARI AML, we report ozone mixing ratio with 1-second time resolution throughout the campaign via UV absorbance measurement [2B Tech]. These data are shown in Figure 21 as both a map of the AML drive track color-coded by ozone mixing ratio, as well as a diurnal time series of all data and 30-minute averages. We note that there was an approximate 30-minute time period on 21-Apr where we observe unexpectedly high and variable ozone mixing ratios during an investigation of point source emissions near Lancaster, TX.

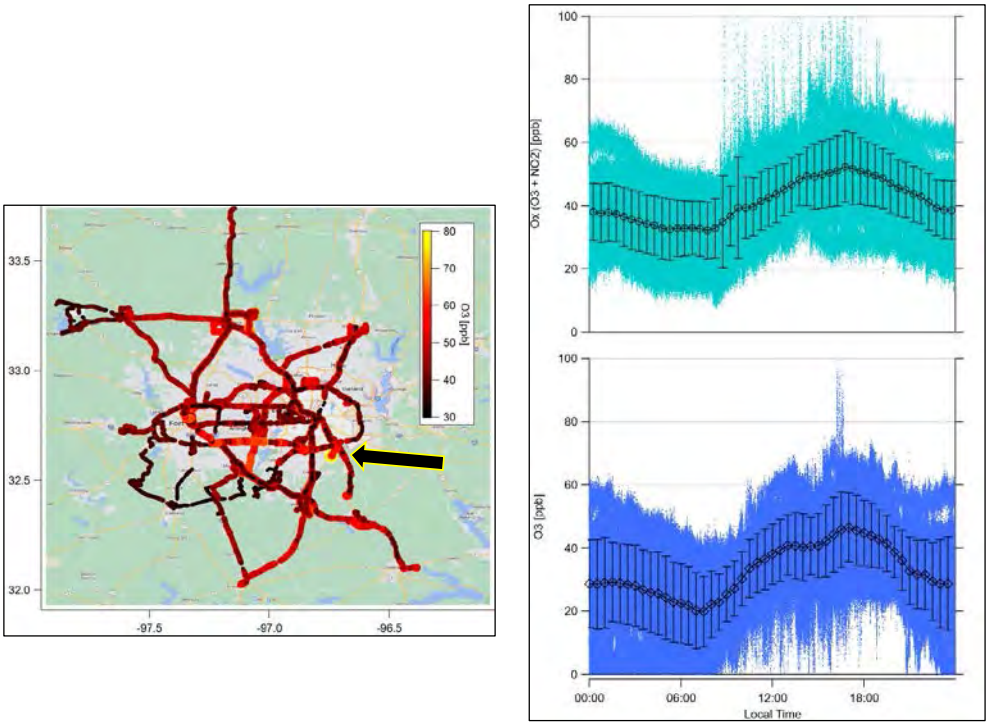

Figure 21. (Left) Map of AML track during DFW AQRP study, color-coded by ozone mixing ratio. (Right) Diurnal time series of ozone (lower) and Ox [=O_3 + NO_2] (upper) mixing ratio measured from AML, showing all 1-second data and 30-minute averages (bars ± 1-σ). The box in right figure shows datapoints of enhanced ozone observed on 21-Apr; the arrow in left figure shows location near Lancaster, TX where this was observed.

As UV-based ozone measurements have a known positive-bias for some aromatic species [Spicer et al., 2010], we evaluated this data for potential interference and found high styrene mixing ratio via GC-EI-TOFMS associated with a point-source plume (Figure 4). Excluding these data, we observed no 1-second ozone mixing ratio >75 ppb and no 1-minute averaged ozone mixing ratio >70 ppb (not shown) for the campaign.

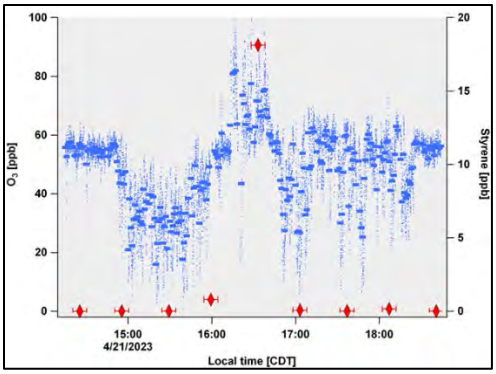

Figure 22. Ozone mixing ratio measured by UV-absorbance from the AML during 21-Apr drive, showing 1-second data (small dots) and 1-minute average data (bars), both in blue. Also shown is styrene mixing ratio (red diamonds) measured via GC-EI-TOFMS, with horizontal bars indicating sample acquisition period.

Upwind – Downwind Experiments

As part of the DFW AQRP study, we used four study days to perform upwind-downwind experiments. Typically, these days involved light but consistent winds that would make point source evaluation more difficult but could allow for multiple hour sampling from a location upwind and then downwind of the metro region. The goal for these experiments was to assess if the relative enhancement in ozone varied as a function of air parcel source or wind direction. Here, we assume that the air parcel will be relatively well-mixed both upwind and downwind of the DFW metro center.

We stationed the AML at the upwind site in the morning to characterize the airmass moving into the metro region, and then moved downwind to evaluate the ozone production that occurred. The experiment days are summarized in Table 4 and maps showing the drives and upwind / downwind locations are shown in Figure 23. Note that the right-most map in Figure 23 shows the drive-track on 17-Apr, as we repeated this drive path on 19-Apr. A time series of 1-minute averaged ozone mixing ratio for a subset of the field campaign is shown in Figure 27 (middle), with the time periods for each upwind and downwind leg indicated by a colored box (blue= upwind, red = downwind).

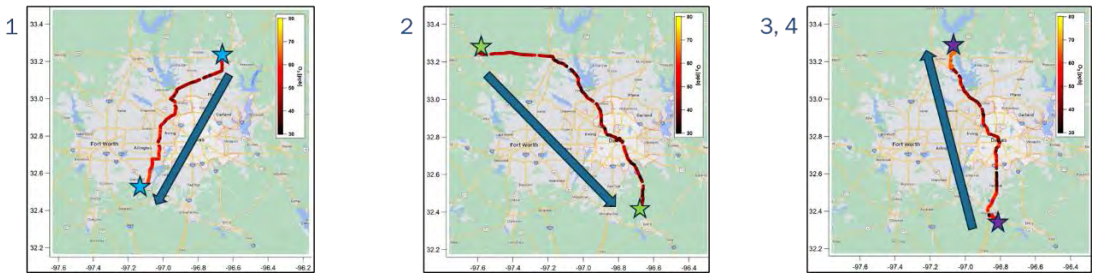

Figure 23. Maps showing AML drive track for upwind / downwind experiments during 2023 DFW AQRP, with drive track color-coded by ozone mixing ratio. General wind direction each day is shown by arrow, locations of stationary sampling points are indicated by stars. Map 1 (8-Apr), Map 2 (16-Apr), Map 3 (17-Apr). Data from 19-Apr not shown but similar to Map 3.

To scale ozone enhancement, here we use co-measured carbon monoxide (CO) mixing ratio to serve as a marker of urban emissions from the metro center. Note that CO was not measured on 19-Apr due to instrumental issues [Figure 27 (bottom)]. For each experiment day with reported mixing ratios for both species, we can compare the relative enhancement of O_3 versus CO as a crude estimate of the O3 production rate that occurred each day. One further detail is that due to the lack of idealized sample locations for these experiments, the measurements were sometimes impacted by local mobile source emissions near the various stationary sites, especially during the upwind sampling on 8-Apr in McKinney, TX. These local emissions can serve to titrate ozone via reaction with emitted nitric oxide (NO).

$$O_3 + NO \rightarrow O_2 + NO_2 \qquad (1)$$

To account for this, we use the sum of ozone and nitrogen dioxide [NO_2] mixing ratios, here called Ox, in place of ozone, assuming that direct emission of NO_2 is relatively insignificant relative to the ambient mixing ratios of O_3 and NO. The time series of Ox mixing ratio is plotted in the top panel of Figure 27. Note that Ox is not subject to overnight titration via Eq (1) above and therefore shows less apparent enhancement each day; the campaign-averaged diurnal ΔO_3 = 26.6 ppb, ΔOx = 19.5 ppb. An important caveat when considering Ox rather than O_3 is that it is possible to have a modest positive bias due to local NO_2 emissions. For example, the maximum 1-hr averaged Ox measurement (71.3 ppb) on 17-Apr, downwind of the metro center at Clear Creek Natural Heritage Center (Denton, TX), is higher than the maximum 1-min averaged O_3 value (70 ppb) at the same location. The time series in Figure 27 for O_3 shows some titration events at the end of that sample period due to local mobile emissions in the parking lot where we sampled, but also some enhancements in Ox likely due to NO_2 emissions from these vehicles.

To evaluate the relative ozone production that occurred each day as the air parcel transected from upwind to downwind, we plot the mixing ratios of Ox and CO for the time periods of interest each day while the AML was holding station at the upwind and downwind sites. These data are shown in Figure 24 below. In each case, the data markers are color-coded by the sum of NO and NO_2 [NOx] to indicate the relative impact of NOx to the sample site. We expect low NOx for the upwind leg, as observed for the 16-Apr and 17-Apr plots, but we can account for local NOx emissions as found on 8-Apr by using Ox in place of O_3 for this work. For each day, we find the slope of Ox to CO via orthogonal distance regression linear fits, which allow us to estimate the enhancement (or production) of O_3 as Ox relative to the enhancement of CO, which is assumed to increase due to emissions alone. These slopes or ratios can be directly compared as they should allow us to account for differences in dilution as a function of distance from the metro center and wind speed.

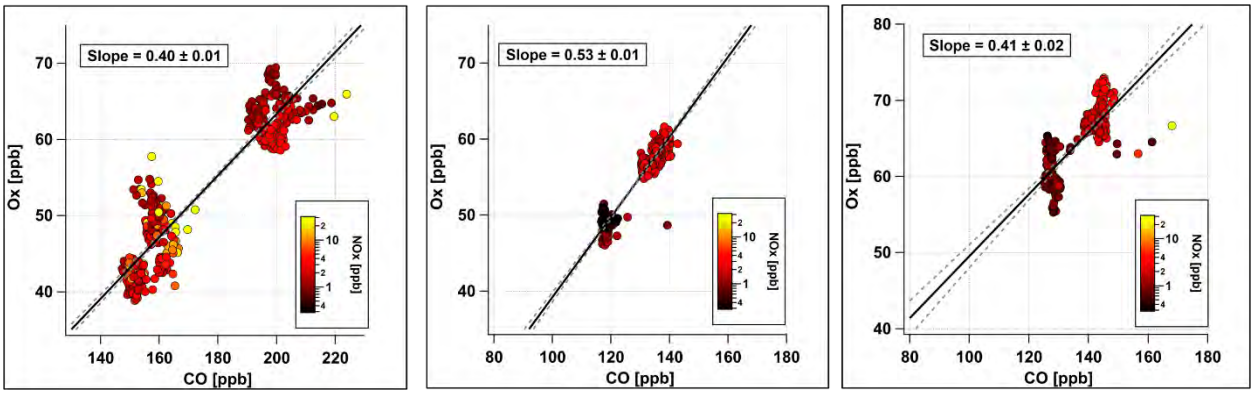

Figure 24. Scatter plots of Ox [= O_3 + NO_2] vs CO for first three upwind / downwind experiments during 2023 DFW AQRP study. Data points are color-coded by NOx [=NO + NO_2] mixing ratio, using a logarithic scaling. Lines represent orthagonal distance regression linear fits for each set of data, with slope and 1-σ uncertainties of slopes shown.

With this analysis, we find that ozone production observed during the first three experiments ranged between 0.40 – 0.53 O_3 per CO, a relatively narrow range. Moreover, the ozone production observed on 8-Apr and 17-Apr are statistically identical within stated uncertainties, despite different wind directions of northwest and south southeast, respectively. We do observe ozone production roughly 25% higher on 16-Apr, where the airmass originated in the northwest and transported on northwest winds. The air temperature on 16-Apr was not especially warm on average during the experiment relative to other days and roughly as humid at 17-Apr (via dew point) although this day was slightly sunnier as measured by solar insolation (Table 4).

To further consider the higher ozone production rate observed for air coming to DFW from the northwest, we can evaluate the VOC species in the air measured both upwind and downwind of the metro area. Figure 25 shows bar charts for some VOC species reported by the GC-EI-TOFMS system while the AML was parked at the sampling locations upwind or downwind for each of the four experiment days. The 17-Apr upwind measurements are from a single datapoint at Spring Park on the north shore of Lake Waxahachie, as other GC samples were flagged for potential contamination by boater activity; all other data is based upon $n \geq 3$ at each location. The upwind 17-Apr sample still shows enhancement in most hydrocarbons more than 1 order of magnitude greater than what was observed two days later at the same site with no boater activity and may need to be removed from the data set.

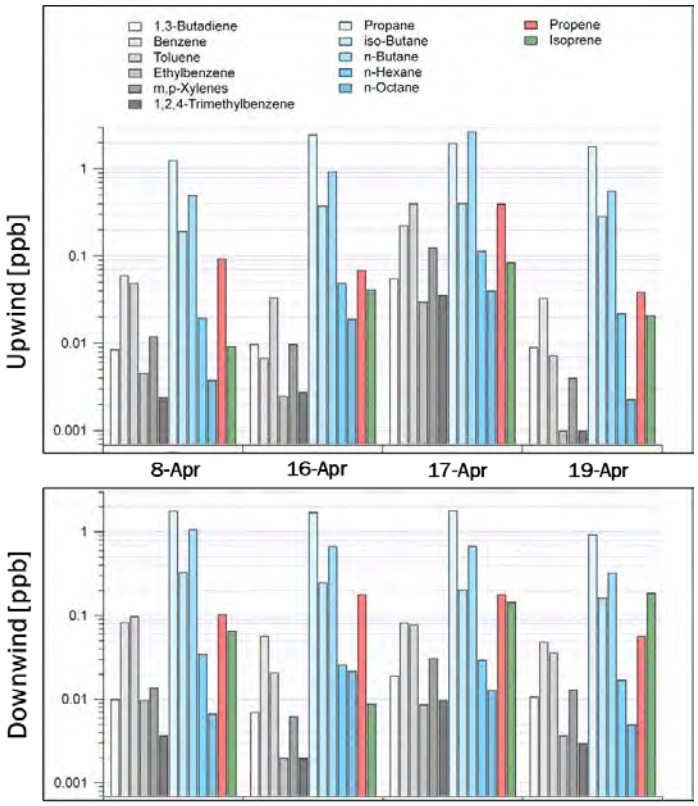

Figure 25. Mixing ratios of select hydrocarbons (aromatics, alkanes, alkenes) measured before ozone production (upwind) and after ozone production (downwind) for the four days of upwind/downwind experiments.

Downwind samples from the four locations show similar mixing ratios after the airmass has passed through the metro area, although the higher O_3 production rate day (by O_3:CO ratio, see above) does show the lowest mixing ratios of the larger and most reactive aromatic species (≥C8; see below). The alkane mixing ratios upwind and downwind each experiment day show smaller changes in absolute mixing ratios and relative concentrations. The higher isoprene concentrations observed at the downwind location on 17-Apr and 19-Apr at Clear Creek Natural Heritage Center (Denton, TX) are likely from local emissions from the oak trees in that park. The upwind airmass observed on 19-Apr had significantly lower concentrations of larger aromatic species (≥C8), and maximum observed 1-minute averaged (Table 4) and 8-hour averaged (Figure 22) mixing ratios of ozone on that day were lower that day than observed for the other three experiment days. Finally, we acknowledge here that further, more sophisticated work via photochemical modeling would be needed to fully explore the differences between experimental days.

A coarse assessment of the photochemical activity for each day can be provided by comparing the ratios of larger and smaller aromatic species (e.g. 1,2,4-trimethylbenzene [1,2,4-TMB] versus toluene), using this ratio change as a photochemical clock. [*Warneke et al.*, 2007]. Simply, since the reaction rate of trimethylbenzene with hydroxyl radical is significantly faster than toluene, we can use the change in the ratio of mixing ratios of these species to estimate the airmass exposure to hydroxyl radical, where exposure is the product of time and hydroxyl radical mixing ratio.

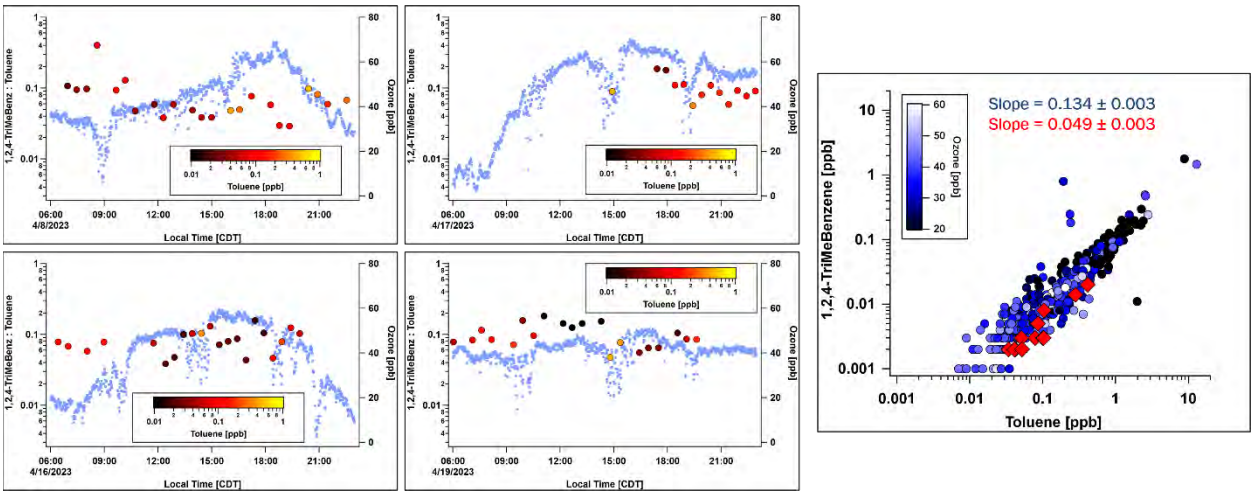

Figure 26. (Left) Time series of ozone and the ratio 1,2,4-Trimethylbenzene : toluene (colored by toluene mixing ratio) for each ambient air GC sample acquired on each upwind / downwind experiment day. (Right) 1,2,4-Trimethylbenzene versus toluene mixing ratio, colored by O_3 mixing ratio for the entire field campaign. Red diamonds represent data from 8-Apr upwind-downwind experiment, showing lower slope than field campaign overall, indicating active photochemistry.

Figure 26 shows how this approach can be applied to the upwind / downwind experiments during the 2023 DFW AQRP study. To determine an estimate of emission ratio for 1,2,4-TMB : toluene, we can plot all measurements of these species for the campaign and solve an orthogonal distance regression linear fit to estimate, relying upon the fact that the largest mixing ratio observations should drive the estimate of the slope. In this case, we find the campaign-wide slope to be 0.134, which represents the emission ratio for these species for the DFW area during the campaign. As an example, we also fit 1,2,4-TMB and toluene mixing ratios from the 8-Apr upwind / downwind experiment (as shown in Figure 8, right). Here, the slope, and therefore 1,2,4-TMB:toluene ratio, is determined to be 0.049, significantly smaller than the emission ratio and an estimate of the hydroxyl radical exposure of the airmass. Slopes for all four experiment days have been calculated via this method (Table 1). The results are unexpected, as the day with smallest perturbation in ratio, and therefore the lowest estimate of hydroxyl radical exposure, is the day with highest ozone mixing ratio and highest estimate of ozone production via O_3:CO ratio.

Further work with additional VOC species measured at the AML via GC-EI-TOFMS and Vocus PTR-TOFMS, along with comparison of the measurements with local AutoGC measurements from TCEQ will be required to evaluate the relative merits of the analyses here.

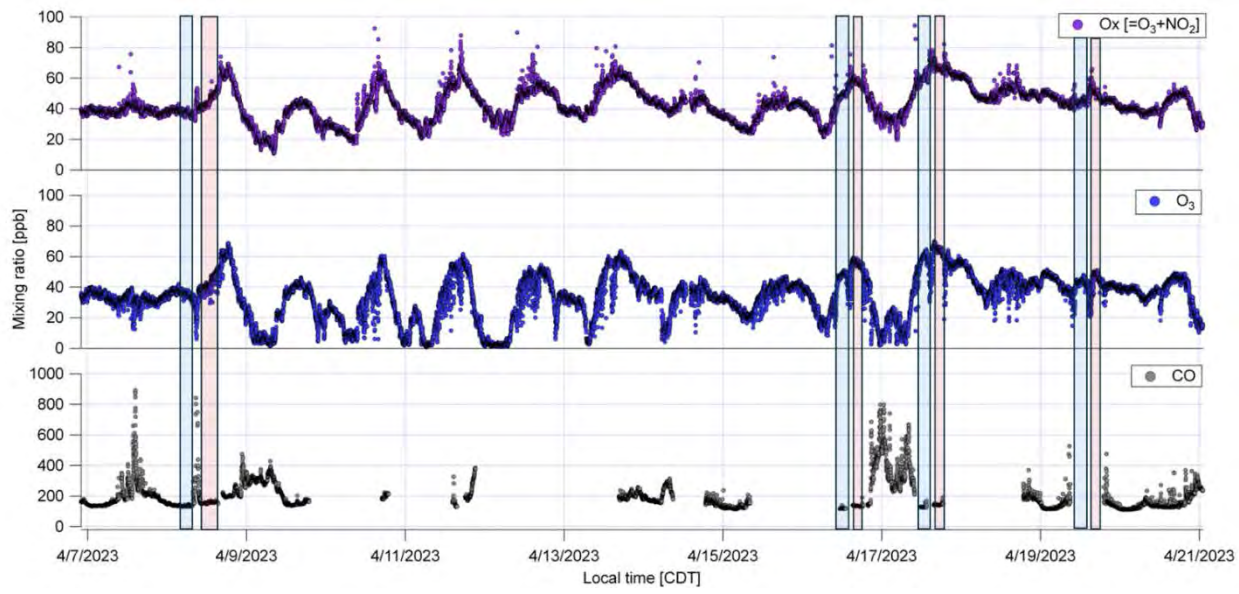

Figure 27. Time series of 1-min averaged Ox, O3 and CO during 2023 DFW AQRP study, showing subset of data surrounding upwind-downwind experiments. Upwind events indicated in blue boxes, downwind legs in red boxes

Date	Upwind (arrival time)	Downwind (arrival time)	Max 1-min O_3 [ppb]	Max 1-hr Ox [ppb]	Ox / CO	Temp [C]	Dew Pt [C]	Solar [Ly/min]	Trimethylbenzene /Toluene
8-Apr (Sat)	McKinney (9:25 CDT)	Mansfield (16:50 CDT)	69	65.3	0.40	20.7	11.5	0.66	0.049 ± 0.003
16-Apr (Sun)	Decatur (10:37 CDT)	Palmer (15:16 CDT)	59	58.8	0.53	20.2	1.3	0.85	0.098 ± 0.006
17-Apr (Mon)	Waxahachie (11:45 CDT)	Denton (15:50 CDT)	70	**71.2**	0.41	24.9	4.7	0.77	0.068 ± 0.011
19-Apr (Wed)	Waxahachie (10:40 CDT)	Denton (16:19 CDT)	51	54.4	-	27.4	18.9	0.49	0.059 ± 0.006

Table 4. Summary of upwind-downwind experiments conducted by Aerodyne AML during 2023 DFW AQRP study. Ox is the sum of O_3 and NO_2, solar insolation in units of Langley/minute. Temperature, dew point and solar insolation data from Meacham Field meteorological station, due to malfunction of data logging for AML AriSense device. Trimethylbenzene/Toluene is the ODR linear regression of 1,2,4-Trimethylbenzene to toluene mixing ratio for the upwind thru downwind time.

Biomass Burning Measurements

One of the primary goals of this project was to measure any biomass burning incident which might occur during the intensive campaign and analyze its interaction with the DFW metropolitan area. During the intensive campaign period of Apr 3 – Apr 23 wildfire conditions in the area were monitored daily (Figure 28). When determining the measurement plan for the next day's activity a number of information sources on line were utilized including https://tfsweb.tamu.edu/CurrentSituation/ and https://www.nifc.gov/fire-information/nfn. Other sites which modeled smoke https://fire.airnow.gov/# and drought conditions in the state of Texas were used for guidance as well https://www.drought.gov/states/texas.

While the primary daily goals were to conduct local measurements (point source and upwind/downwind) the option of going to a wildland fire and conducting measurements was considered daily. As Figure 28 depicts during the time that measurements were conducted there were very few if any opportunities to measure wildland burning within a reasonable distance to DFW metropolitan area which could be expected to impact DFW metropolitan area air quality. The closest fires to the DFW metropolitan area were actually in central Oklahoma and the decision was made to sample the Swine Fire near Wewoka OK on Apr 22. This fire at one point was reported up to 10,000 acres total extent but by the time the AML visited the area the fire was primarily light smoldering (Figure 29). Measurements of this fire were conducted for approximately 1 ½ hours before the AML transited back to the DFW area. There were north winds during the time period the AML sampled in DFW and it is certainly possible that smoke from the Swine Fire did move downstream into DFW but it would have been a very minor component of the overall air quality given the fires small size and large transport distance.

Figure 28. Map of Texas depicting locations where wildfires occurred from Apr 3 – Apr 23. The red markings are areas of burning.

Figure 29. Picture of area burned by fire near Wewoka OK

One analysis tool that can be used to compare the signal seen at the fire with measurements at DFW over the course of the campaign is Positive Matrix Factorization (PMF)[*Ulbrich et. al.* 2009] of the organic aerosol measured with the SP-AMS. PMF has been conducted on both the smaller fire dataset and the large 3-week intensive campaign. A factor for the overall campaign is selected which most closely resembles the factor obtained at the burn site (Figure 30) and the presence of that factor over time is depicted in Figure 31. It is noteworthy that there is a significant biomass burning factor on both Apr 9 and to a lesser extent Apr 17 in DFW.

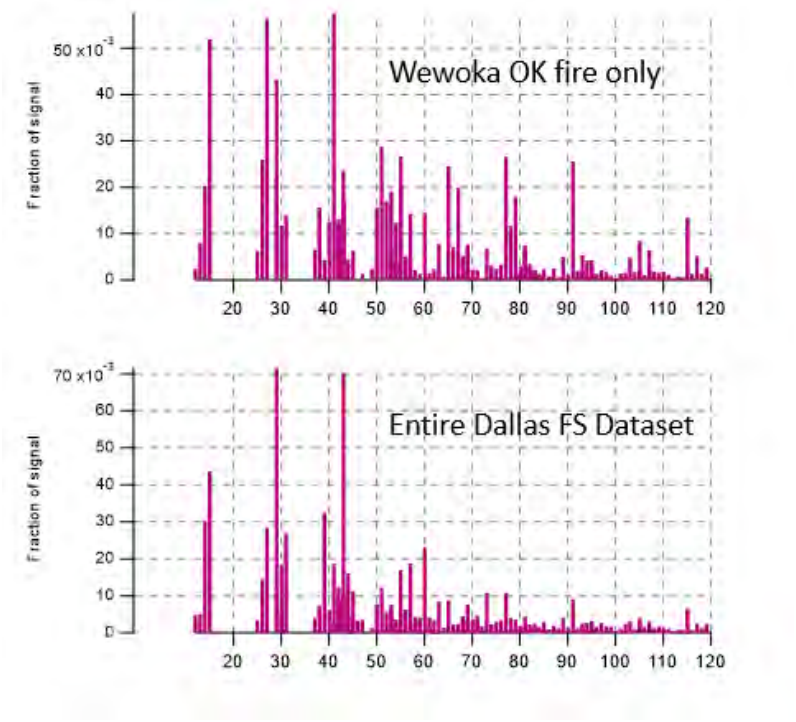

Figure 30. The biomass burning factor derived by PMF for the burn only at top and for the overall campaign at bottom.

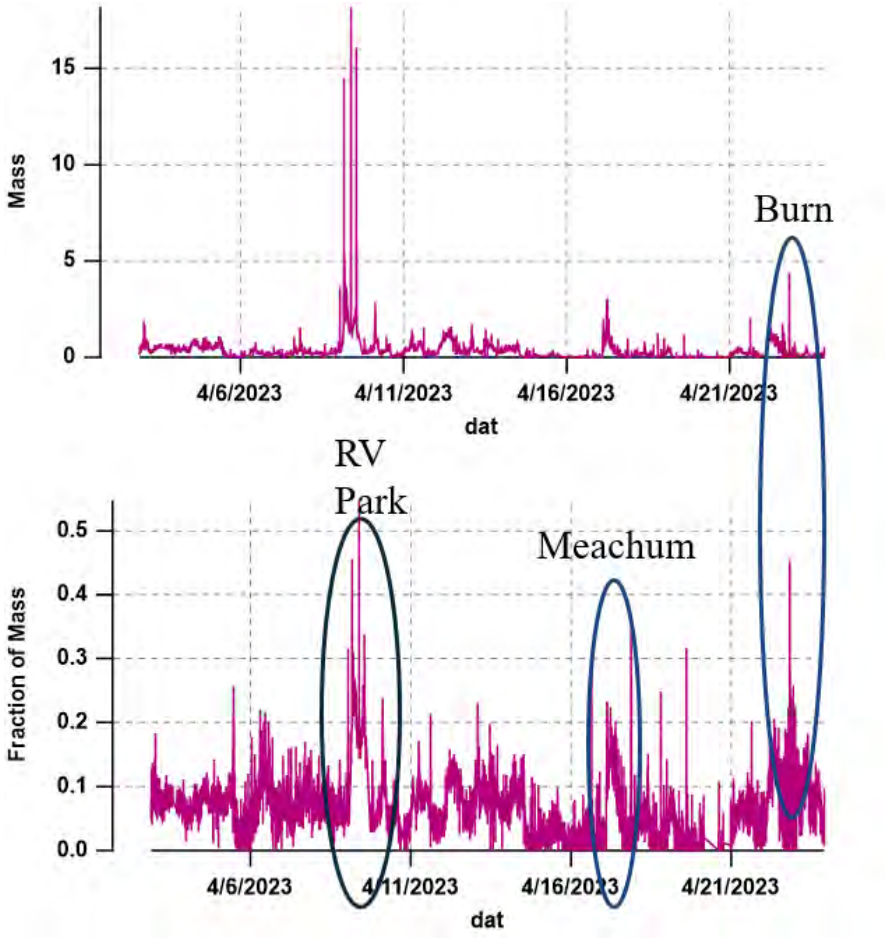

Figure 31. The biomass burning factor derived by Positive Matrix Factorization (PMF) shows over time total loading at top and fractional contribution at bottom. Note elevated factor levels on April 9 and April 17 while at the Texan Ranch RV Park and Meachum Field respectively.

Fort Worth Northwest Stationary Site Meachum Field

Intercomparisons

During the Dallas Field Study, the AML was stationed at Meachum Field, collocated with the TCEQ's "Fort Worth Northwest" monitoring site. This site is EPA site number 484391002 and CAMS site number 0013 and is located at GPS coordinates of (32.8058182, -97.3565229). TCEQ measurements include meteorology (wind, temperature, solar radiation, relative humidity, and dew point), $PM_{2.5}$, ozone and NOx, and a variety of VOCs measured via AutoGC and canister samplers. TCEQ data from this site is available at: https://www17.tceq.texas.gov/tamis/index.cfm?fuseaction=report.view_site&siteAQS=484391002

Two AQRP-funded and one TCEQ-funded project operated out of the Fort Worth Northwest site during the Spring 2023 measurement period. In this measurement year, TCEQ funded the expansion of the (BC)2 network to this site. This project, led by Baylor University PIs, aims to measure biomass burning signatures in Texas. Black Carbon and Brown Carbon (hence $(BC)^2$) are quantified using optical absorption and scattering methods. The current project, AQRP 22-010, funded a full mobile laboratory deployment for 3 weeks, which was based out of this site when not mobile. Finally, a second AQRP project, AQRP 22-060, funded the additional measurement of HCN at the expanded (BC)2 network site for 2 months.

Below, we show data from the Fort Worth Northwest site for the duration of the DFS. Select measurements from all three platforms are shown: the TCEQ trailer (wind speed and direction), the (BC)2 trailer (HCN) (green), AAE: Absorption Angstrom Exponent (365-640nm) and SAE: Scattering Angstrom Exponent (450-635nm), and the AML (all other tracers, including a secondary HCN measurement, purple)

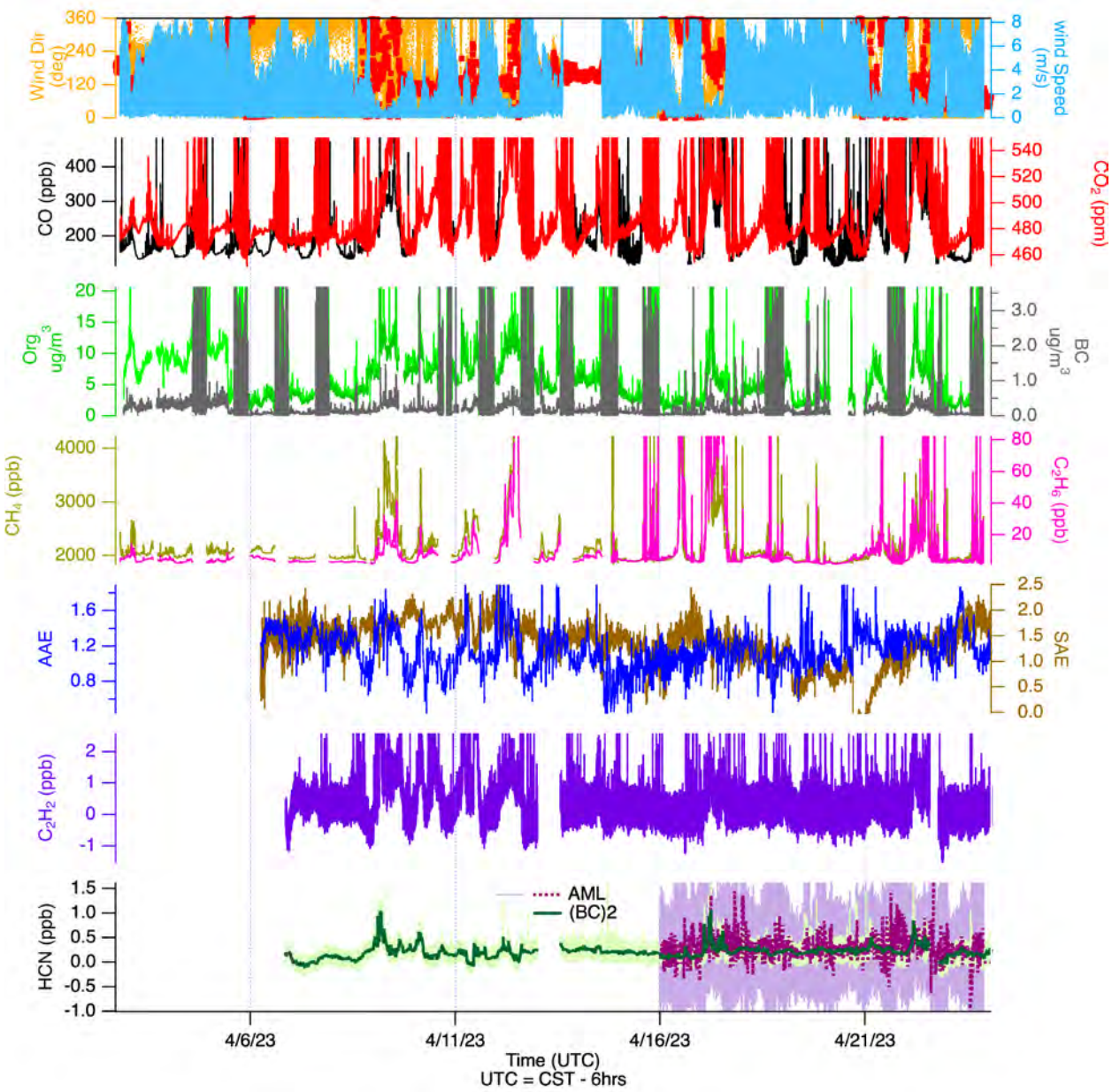

Figure 32. Select biomass burning tracers at the Fort Worth Northwest site. Data shown on this plot includes measurements from the AML (AQRP 23-010), the (BC)2 network trailer (Baylor TCEQ project, and AQRP 23-060) and the TCEQ trailer. HCN data is shown at 1-second time scale (pale green and pale purple) and at 5-minutes (bold green and dotted purple traces). (BC)^2 project data is preliminary and confidential.

We see a favorable comparison of AML wind data with TCEQ site wind data, showing discrepancies, as expected, when the AML was mobile or away from the site. No consistent bias in wind speed or direction is noted.

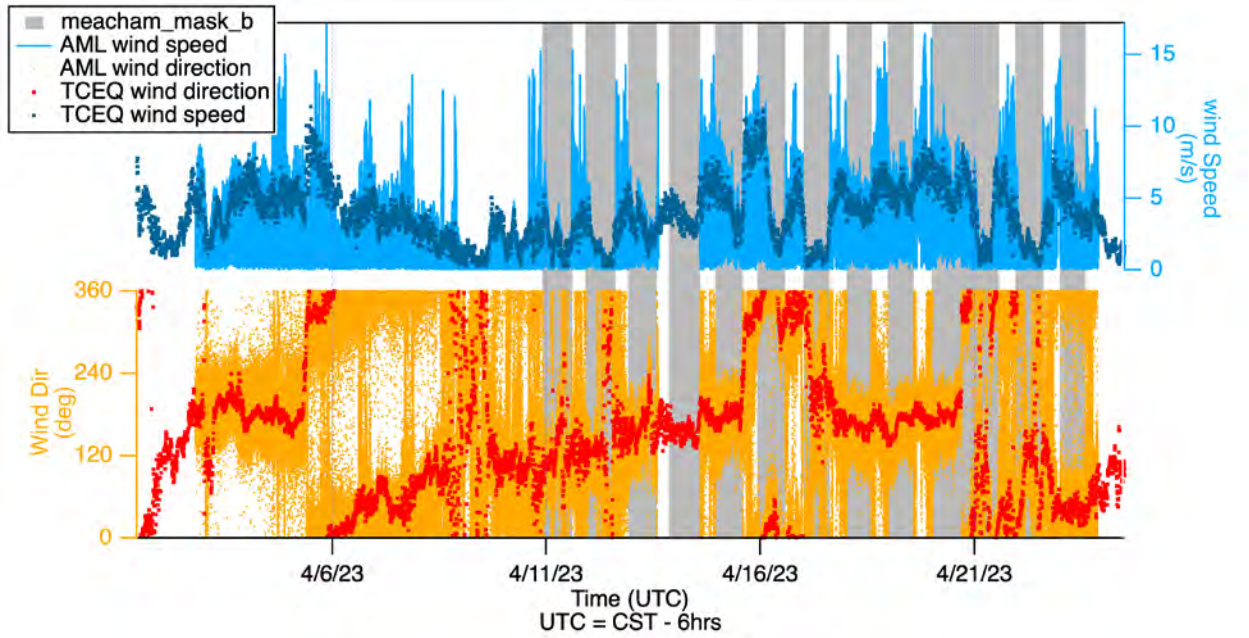

Figure 33. Comparison of wind measurements between the AML and the TCEQ Fort Worth Northwest site. Shaded areas indicate times when the AML was at the TCEQ site.

Next, we compare HCN measurements between the AML instrument (purple) and the HCN instrument installed in the (BC)2 trailer (green) as part of AQRP-060 project (Figure 32). Here, HCN data from the AML start on 4/16/2023, when an inlet leak was fixed (see TILDAS QA document). This period was chosen since lengthy refits were necessary, and so this known high quality time period was prioritized. Additional refits to recover stationary measurements prior to this time could be done, but as discussed in the QA document, would still be subject to an unknown time constant due to the mixing in of truck cab air.

The data is filtered to include only measurements taken at the Dallas Fort-Worth site, and the 5-minute average is taken. The AML HCN trace is about 10% low compared to the calibrated output of the HCN instrument in the $(BC)^2$ trailer. No calibration factor has yet been applied to the AML HCN, however. Both instruments had calibrations done with the same calibration tank. Future data revisions will report calibrated data.

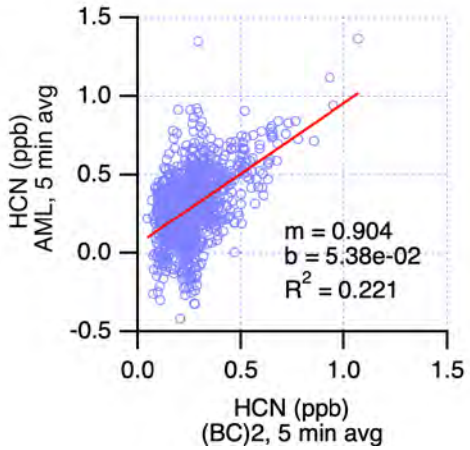

Figure 44. Comparison of uncalibrated AML HCN data to calibrated HCN data from the $(BC)^2$ trailer

Next, we examine time series between 4/16 to 4/23 and exclude periods when the AML was measuring point sources. The majority of the time, activity in biomass burning tracers was fairly quiet, as can be seen in the graph below. This is a stationary period on the final overnight of the campaign. In this graph, the shaded tracers indicate data collected in the $(BC)^2$ trailer, unless noted.

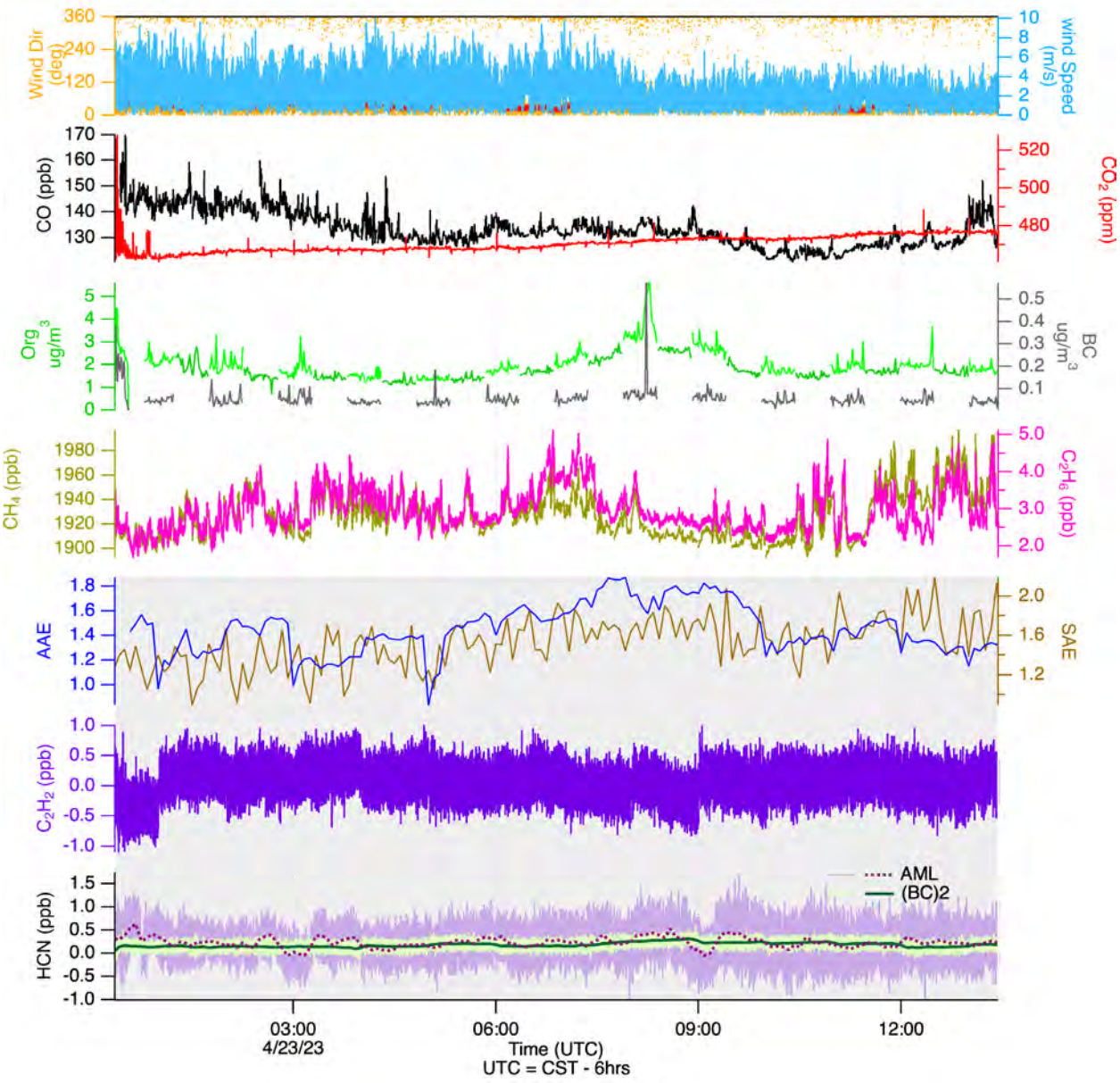

Figure 35. Select biomass burning tracers at the Fort Worth Northwest site. Data shown on this plot include measurements from the AML (AQRP 23-010), the (BC)2 network trailer (Baylor TCEQ project, and AQRP 23-060) and the TCEQ trailer. HCN data is shown at 1-second time scale (pale green and pale purple) and at 5-minutes (bold green and dotted purple traces). The shaded tracers indicate data collected in the $(BC)^2$ trailer, unless noted. $(BC)^2$ project data is preliminary and confidential.

However, there were instances of suspected biomass burning influence. In the graph below, we highlight one period. This is indicated by a concomitant enhancement in CO, organic particulate matter, and HCN for the plume appearing at 4/17/23 05:30 – 06:00 UTC (4/16/23 23:30 – 4/17/23 00:00 CST). AAE is also elevated above 1. The report for AQRP 22-060 will detail the identification of biomass burning plumes using the full suite of parameters measured at the $(BC)^2$ site.

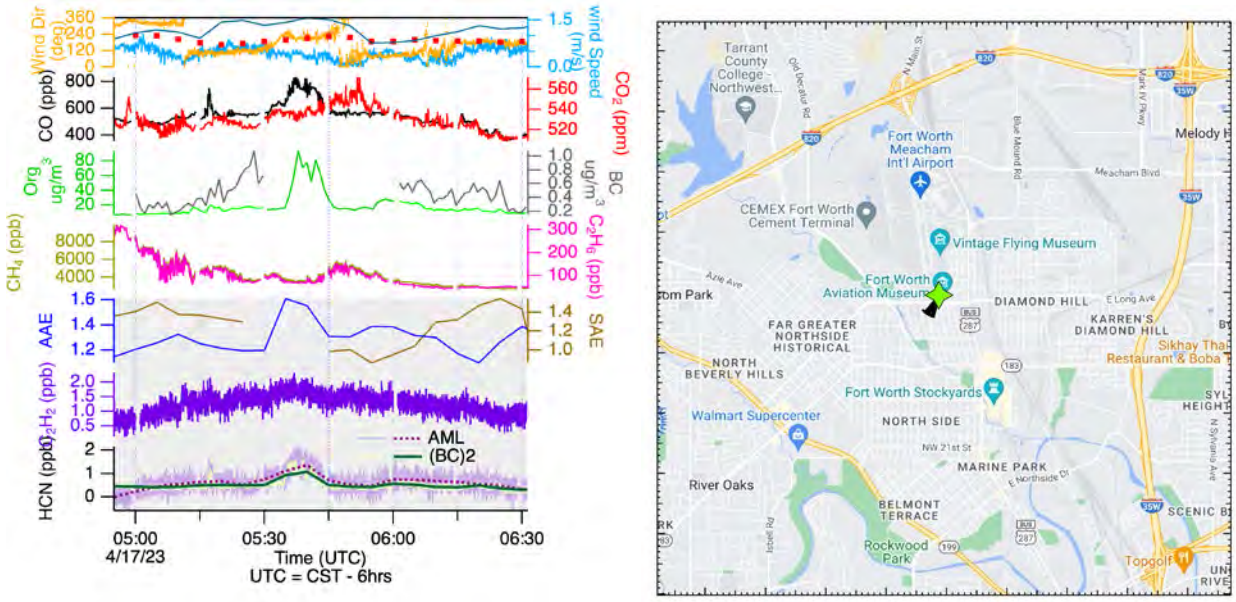

Figure 36. Time series (left) showing a potential biomass burning plume between 05:30 and 06:00 UTC. Enhancements in several Biomass Burning (BB) tracers are observed, including HCN (measurements aboard the AML, green, and inside the $(BC)^2$ trailer, purple), AAE, Organic PM and CO. Shaded traces are from the $(BC)^2$ trailer unless otherwise noted. TCEQ-measured wind (5 min data) is shown alongside AML-measured wind (1 second data). A map (right) showing the location of the Fort Worth Northwest site (green star) with wind barbs (black) indicating a wind from the southwest.

Meachum Field Runway Considerations

Between mobile sampling periods, the Aerodyne Mobile Laboratory occasionally collected stationary data downwind of aircraft activity (landing, idling, take-off – 'LTO') at Fort Worth Meacham International Airport. Approximately 500 m away from the nearest runway, the AML typically parked facing south from the late afternoon to early morning (Figure 37). Winds out of the northwest to north were considered likely to bring LTO emissions from a collection of mostly single-piston aircraft (e.g., Cessna 172, Piper PA-28).

Figure 37. Partial map of Fort Worth Meacham International Airport showing the proximity and direction of aircraft runways relative to the stationary sampling site location (yellow star) – approximately 500 m north northwest. Map data from OpenStreetMap.

Some chemical compounds associated with aircraft emissions include NOx, CO, CO_2, and HCHO. Concentration roses of HCHO and NOx in Figure 38 show enhanced emissions from the direction of the runway (north northwest) for stationary periods with elevated wind speeds (3 m s^{-1}). Engine type influences the emissions profile, which changes across operational modes (idle, take-off) at different combustion temperatures. Idle exhaust plumes containing HCHO and CO have been observed in a ratio of 21 ± 8 pptv $ppbv^{-1}$ at Hartsfield-Jackson Atlanta International Airport (*Herndon et al*., 2008b).

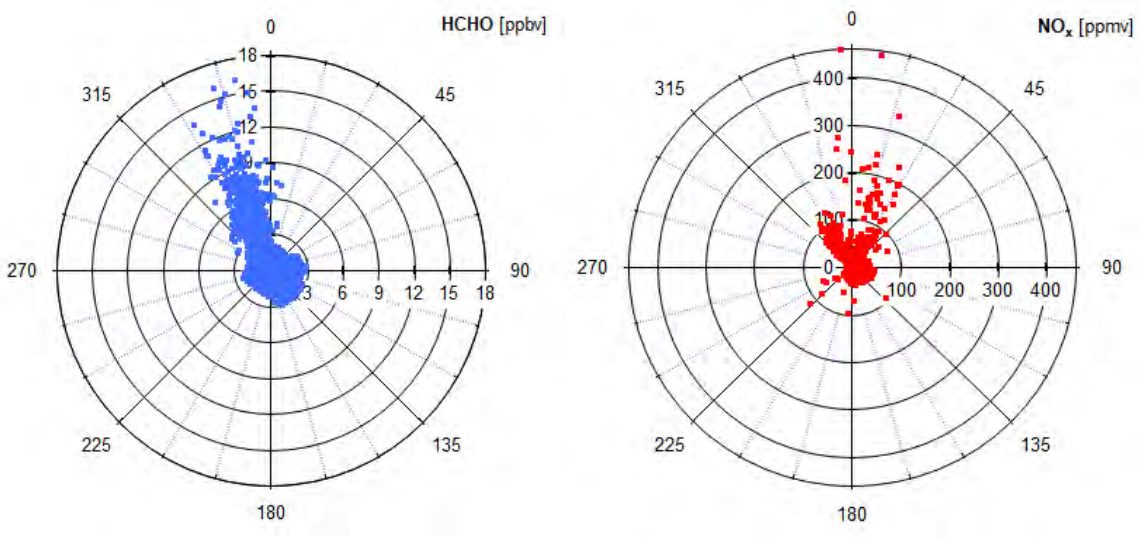

Figure 38. Concentration rose for formaldehyde (ppbv) and nitrogen oxides (ppmv) during periods of stationary measurements at Fort Worth Meacham International Airport (wind speed > 3 m s^{-1}) between April 11 – April 23, 2023.

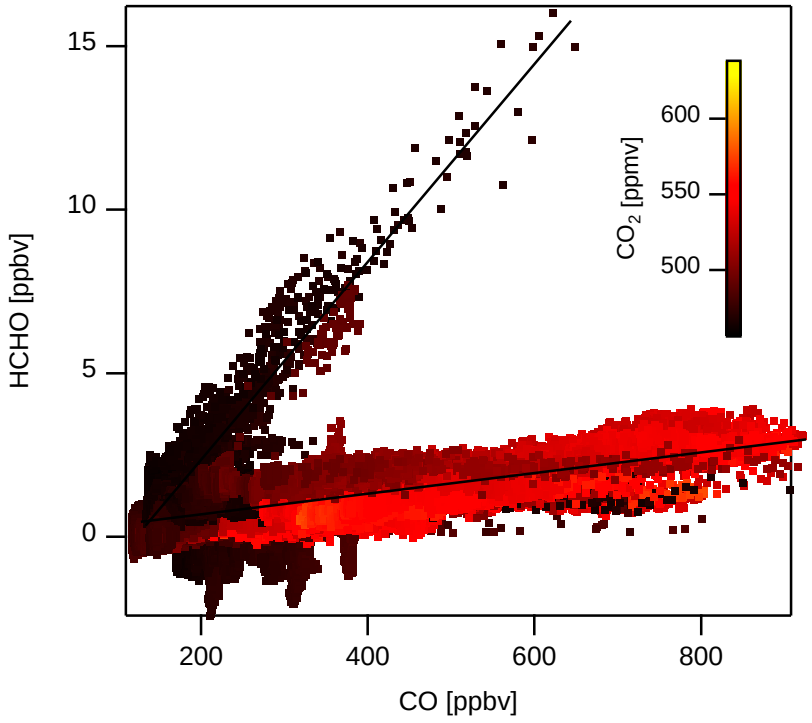

Figure 39. Concentration of formaldehyde (ppbv) relative to carbon monoxide (ppbv) during periods of stationary measurements at Fort Worth Meacham International Airport (wind speed > 3 m s^{-1}) between April 11 – April 23, 2023. Ratios have been colored by CO_2 (ppmv) concentration as an indication of dilution. Linear trend lines represent two unique clusters of data.

Concentration ratios of HCHO (ppbv) to CO (ppbv) appear in two distinct data clusters (Figure 39) during this sample period (stationary, wind speed > 3 m s^{-1}). A linear trend line drawn through one population is roughly 20 pptv $ppbv^{-1}$ which resembles the previously mentioned observations of aircraft engine idling. A second cluster follows a trend of 3 pptv $ppbv^{-1}$ and appears to be associated with less diluted emissions (based on higher relative CO_2 values), which could be from nearby diesel vehicle emissions (the AML or its generators) or other types of aircraft activity (takeoff and departures).

On a no-drive day (4/20/23), the AML sampled emissions from the direction of the runway during the middle of the day. One example shows closely correlated enhancements of HCHO and CO (~25 pptv $ppbv^{-1}$) along with mildly correlated NOx (Figure 40), lasting a few minutes. Given the prolonged duration of the plume and HCHO:CO ratio, it appears likely that these emissions could be from idling aircraft on the runway. Flight records from the airport could help corroborate these findings.

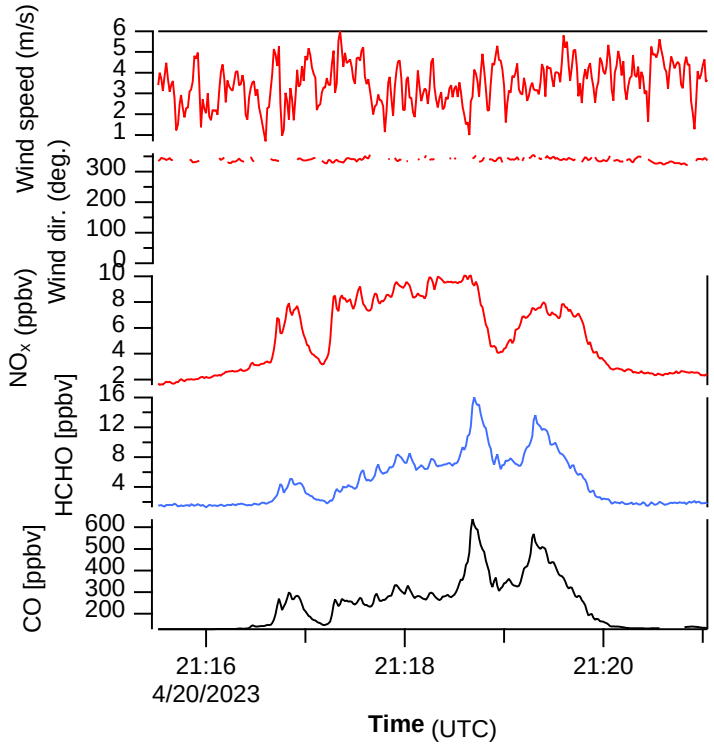

Figure 40. Time series of emissions (CO, HCHO, NOx) and wind conditions (speed and direction) during a stationary measurement period downwind of the Fort Worth Meacham International Airport.

Conclusions

The AML sampled over 50 point sources in the DFW area and gained a wealth of information regarding the chemical speciation of the gas and particle phase emissions from those facilities. The different VOC makeup among different sources leads to different OH reactivities among facilities. It is useful to have knowledge of the chemical makeup of these VOC emissions and more thorough modeling in the future would enhance the ability to infer O_3 production related to these emissions. The upwind/downwind measurements were also quite useful to see the effect of the urban DFW area on airmasses and modeling using this input data in the future would be useful as well. Biomass burning was sampled and a biomass burning factor related to organic aerosol emissions was found from the burn and can be applied to the Dallas FS measurements of organic aerosol throughout the measurement period. Intercomparisons were conducted between the Baylor Trailer associated with AQRP Project# 22-060 and the AML, and HCN was detected on both platforms associated with biomass burning influence detected at Meachum Field on at least one day. A study of the stationary signal while at Meachum indicated that knowledge of the exact takeoff and landing history at the airfield would be useful both for a QC check of data at Meachum Field and as a measurement of a known aircraft emission including the type of aircraft.

In considering the best method for studying wildfires which may occur in the future it would be beneficial to have the ability to deploy to a specific wildfire area of interest more rapidly. This campaign has many resources that are in high demand, and it becomes necessary at some point to fix a schedule which may or may not be in a time of high fire activity. If it were possible to have a standby measurement platform with the flexibility to deploy only when conditions are favorable that would be ideal.

Acknowledgements:

The efforts of Dakota Shaw at Fort Worth Meachum Field, Vince Torres, RoseAnna Goeway of AQRP, Sascha Usenko at Baylor and the TCEQ team towards obtaining the necessary infrastructure and clearances to base out of Meachum Field are greatly appreciated. The employees of Texan RV Ranch are also greatly appreciated for their hospitality during our stay there.

References:

Anderson, D. C., J. Pavelec, C. Daube, S. C. Herndon, W. B. Knighton, B. M. Lerner, J. R. Roscioli, T. I. Yacovitch, and E. C. Wood (2019), Characterization of ozone production in San Antonio, Texas, using measurements of total peroxy radicals, *Atmos. Chem. Phys.*, *19*(5), 2845-2860, doi:10.5194/acp-19-2845-2019

census.gov (Accessed 08/11/22) Metropolitan and Micropolitan Statistical Areas Totals: 2020-2021 (census.gov)

Domínguez, R. M., Arturo, D., & Trejo, R. (2004). Forest Fires in Mexico and Central América. *Proceedings of the Second International Symposium on Fire Economics, Planning, and Policy: A Global View*, *5*, 709–720.

Current Texas Drought Map (Accessed periodically 01/01/23 – 04/30/23) www.drought.gov/states/texas

Fire and Smoke Map (Accessed periodically 01/01/23 – 04/30/23) https://fire.airnow.gov/#

Gilman, J. B., Lerner, B. M., Kuster, W. C., Goldan, P. D., Warneke, C., Veres, P. R., Roberts, J. M., de Gouw, J. A., Burling, I. R., and Yokelson, R. J.: Biomass burning emissions and potential air quality impacts of volatile organic compounds and other trace gases from fuels common in the US, Atmos. Chem. Phys., 15, 13915–13938, https://doi.org/10.5194/acp-15-13915-2015, 2015.

Herndon, S. C., et al. (2008), Correlation of secondary organic aerosol with odd oxygen in Mexico City, *Geophys. Res. Lett.*, *35*(15), L15804, doi:10.1029/2008GL034058.

Herndon, Scott C., et al (2008b). "Commercial aircraft engine emissions characterization of in-use aircraft at Hartsfield-Jackson Atlanta International Airport." *Environmental science & technology* 42.6: 1877-1883.

Manion, J. A., Huie, R. E., Levin, R. D., Burgess Jr., D. R., Orkin, V. L., Tsang, W., McGivern, W. S., Hudgens, J. W., Knyazev, V. D., Atkinson, D. B., Chai, E., Tereza, A. M., Lin, C. J., Allison, T. C., Mallard, W. G., Westley, F., Herron, J. T., Hampson, R. F., and Frizzell, D. H.: NIST Standard Reference Database 17, Version 7.0, http://kinetics.nist.gov/, last access: 11 November 2015, 2015.

Massoli, P., et al. (2012), Pollution Gradients and Chemical Characterization of Particulate Matter from Vehicular Traffic near Major Roadways: Results from the 2009 Queens College Air Quality Study in NYC, *Aerosol Sci. and Technol.*, *46*(11), 1201-1218, doi:DOI: 10.1080/02786826.2012.701784.

National Interagency Fire Center (Accessed periodically 01/01/23 – 04/30/23) https://www.nifc.gov/fire-information/nfn

Peppler, R. A., Bahrmann, C. P., Ashford, L., Ferrare, R. A., & Halthore, R. N. (1999). Identification and Analysis of the 1998 Central American Smoke Event at the ARM SGP CART Site Large-Scale Environment of the Smoke Event. *Science, May 1998*, 1–16.

Santoni, G. W., B. H. Lee, E. C. Wood, S. C. Herndon, R. C. Miake-Lye, S. C. Wofsy, J. B. McManus, D. D. Nelson, and M. S. Zahniser (2011), Aircraft Emissions of Methane and Nitrous Oxide during the Alternative Aviation Fuel Experiment, *Environ. Sci. Technol.*, *45*(16), 7075-7082, doi:10.1021/es200897h.

Spicer, C. W., D. W. Joseph,W. M. Ollison (2010) A Re-Examination of Ambient Air Ozone Monitor Interferences, Journal of the Air & Waste Management Association, 60:11, 1353-1364, DOI: 10.3155/1047-3289.60.11.1353

tceq.gov Point Source Emissions Inventory (2022) www.tceq.texas.gov/airquality/point-source-ei/psei.html

tceq.gov Acency Activities Air Quality (2020) https://www.tceq.texas.gov/publications/sfr/tceq-biennial-report/biennial-report-to-the-87th-legislature-fy2019-fy2020/agency-activities-air-quality

tceq.gov Agency Activities (2022) https://www.tceq.texas.gov/publications/sfr/tceq-biennial-report/biennal-report/chapter-2-agency-activities

tceq.texas.gov Fort Worth Northwest (Accessed periodically 04/01/23 – 08/31/23) https://www17.tceq.texas.gov/tamis/index.cfm?fuseaction=report.view_site&siteAQS=484391002

tfsweb.tamu.edu Current Wildfire Activity (Accessed periodically 01/01/23 – 04/30/23) https://tfsweb.tamu.edu/CurrentSituation/

Ulbrich, I. M., Canagaratna, M. R., Zhang, Q., Worsnop, D. R., and Jimenez, J. L.: Interpretation of organic components from Positive Matrix Factorization of aerosol mass spectrometric data, Atmos. Chem. Phys., 9, 2891–2918, https://doi.org/10.5194/acp-9-2891-2009, 2009.

Van Der Werf, G. R., Randerson, J. T., Giglio, L., Collatz, G. J., Kasibhatla, P. S., & Arellano, A. F. (2006). Interannual variability in global biomass burning emissions from 1997 to 2004. *Atmospheric Chemistry and Physics*, *6*(11), 3423–3441. https://doi.org/10.5194/acp-6-3423-2006

Warneke, C., et al. (2007), Determination of urban volatile organic compound emission ratios and comparison with an emissions database, *J. Geophys. Res.*, 112, D10S47, doi:10.1029/2006JD007930.

Wood, E. C., et al. (2009), A case study of ozone production, nitrogen oxides, and the radical budget in Mexico City, *Atmos. Chem. Phys.*, *9*(7), 2499-2516.

Yacovitch, T. I., S. C. Herndon, G. Pétron, J. Kofler, D. Lyon, M. S. Zahniser, and C. E. Kolb (2015), Mobile Laboratory Observations of Methane Emissions in the Barnett Shale Region, *Environ. Sci. Technol.*, *49*(13), 7889-7895, doi:10.1021/es506352j.

Yokelson, R. J., Crounse, J. D., DeCarlo, P. F., Karl, T., Urbanski, S., Atlas, E., Campos, T., Shinozuka, Y., Kapustin, V., Clarke, A. D., Weinheimer, A., Knapp, D. J., Montzka, D. D., Holloway, J., Weibring, P., Flocke, F., Zheng, W., Toohey, D., Wennberg, P. O., … Shetter, R. (2009). Emissions from biomass burning in the Yucatan. *Atmospheric Chemistry and Physics*, *9*(15), 5785–5812. https://doi.org/10.5194/acp-9-5785-2009